THE GEOLOGICAL SOCIETY OF AMERICA®

Nature of Cretaceous dolerite dikes with two distinct trends in the Damodar Valley, eastern India: Constraints on their linkage to mantle plumes and large igneous provinces from $^{40}Ar/^{39}Ar$ geochronology and geochemistry

Rajesh K. Srivastava[1,*], Fei Wang[2,3,4], Wenbei Shi[2], Anup K. Sinha[5], and Kenneth L. Buchan[6]

[1]CENTRE OF ADVANCED STUDY IN GEOLOGY, INSTITUTE OF SCIENCE, BANARAS HINDU UNIVERSITY, VARANASI 221005, INDIA
[2]STATE KEY LABORATORY OF LITHOSPHERIC EVOLUTION, INSTITUTE OF GEOLOGY AND GEOPHYSICS, CHINESE ACADEMY OF SCIENCES (CAS), BEIJING 100029, P.R. CHINA
[3]CAS CENTRE FOR EXCELLENCE IN TIBETAN PLATEAU EARTH SCIENCES, BEIJING 100101, P.R. CHINA
[4]COLLEGE OF EARTH AND PLANETARY SCIENCES, UNIVERSITY OF CHINESE ACADEMY OF SCIENCES, BEIJING 100049, P.R. CHINA
[5]DR. K.S. KRISHNAN GEOMAGNETIC RESEARCH LABORATORY, INDIAN INSTITUTE OF GEOMAGNETISM, ALLAHABAD 211505, INDIA
[6]273 FIFTH AVENUE, OTTAWA, ON K1S 2N4, CANADA

ABSTRACT

Two distinct sets of Cretaceous dolerite dikes intrude the Chhotanagpur gneissic complex of eastern India, mostly within the Damodar Valley Gondwanan sedimentary basins. One dike set trends NNE to ENE, whereas the other set, which includes the prominent Salma dike, trends NW to NNW. One dike from each set in the Raniganj Basin was dated using the $^{40}Ar/^{39}Ar$ method in order to resolve a controversy concerning the emplacement age of the Salma dike. The NE-trending dike yielded a plateau age of 70.5 ± 0.9 Ma, whereas the NNW-trending Salma dike is much older, with a plateau age of 116.0 ± 1.4 Ma. These results demonstrate that the Salma dike was emplaced at ca. 116 Ma and not at ca. 65 Ma, as suggested in an earlier study. Geochemical characteristics of the two dikes are also distinct and indicate that they belong to previously identified high-Ti and low-Ti dolerite groups, respectively. The observed geochemical characteristics of both dike sets are comparable with the geochemistry of basalts of the Kerguelen Plateau, Bunbury Island, and Rajmahal Group I and suggest a connection to mantle plumes. The new age data presented herein indicate that these two magmatic episodes in the eastern Indian Shield were related to the ca. 120–100 Ma Kerguelen mantle plume and its associated Greater Kerguelen large igneous province and the ca. 70–65 Ma Réunion plume and its associated Deccan large igneous province, respectively.

LITHOSPHERE; v. 12; no. 1; p. 40–52 | Published online 12 December 2019 https://doi.org/10.1130/L1108.1

INTRODUCTION

Due to their vertical depth and lateral extent, mafic dike swarms often survive when the volcanic component of short-lived, mantle-generated magmatic events or large igneous provinces is lost to erosion. Therefore, the study of dikes is of great importance in determining the original extent of large igneous provinces and in linking these events to mantle plumes (Ernst and Buchan, 2001a, 2001b; Bleeker and Ernst, 2006; Ernst et al., 2010; Srivastava et al., 2010, 2019a; Ernst, 2014). Precise age determinations are essential for identifying components of a large igneous province, determining its source plume, and comparing ages of magmatic events on different cratonic blocks (i.e., magmatic barcoding) to test continental reconstructions (e.g., Bleeker, 2003, 2004; Bleeker and Ernst, 2006; Srivastava et al., 2010, 2019a; Ernst, 2014).

The Indian Shield has experienced a number of intraplate mafic magmatic events with ages ranging from Archean to Cretaceous (Kent et al., 1997, 1998, 2002; Srivastava and Sinha, 2004a, 2004b; Paul, 2005; Srivastava et al., 2008a, 2008b, 2014; Srivastava and Ahmad, 2008, 2009; Srivastava, 2011; Samal et al., 2019; and references therein). Although four plume heads (Crozet, Kerguelen, Marion, and Réunion) are thought to have passed under the Indian Shield during the Cretaceous, the major episodes of mafic magmatism observed during this period in the Indian Shield are associated with either the 70–65 Ma Réunion (cf. Courtillot et al., 1988; Chenet et al., 2007; Hooper et al., 2010; Chalapathi Rao and Lehmann, 2011) or 120–100 Ma Kerguelen (cf. Storey et al., 1992; Baksi, 1995; Kent et al., 1997, 2002; Coffin et al., 2002; Ghatak and Basu, 2011; Srivastava et al., 2014; Olierook et al., 2017) plumes. Very little or no magmatism is known for the Crozet and Marion plumes (Curray and Munasinghe, 1991; Roy, 2004). The Réunion plume was active in the western parts of the Indian Shield and produced the Deccan large igneous province (cf. Chenet et al., 2007; Hooper et al., 2010; Ernst,

Rajesh Srivastava http://orcid.org/0000-0003-0549-6597
*rajeshgeolbhu@gmail.com

2014; Mukherjee et al., 2017; and references therein). The Kerguelen plume was most active in the eastern Indian Shield, particularly in the Chhotanagpur gneissic complex (CGC) and the Shillong Plateau (e.g., Rajmahal-Sylhet tholeiitic basalts and mafic dikes; Storey et al., 1992; Baksi, 1995; Kent et al., 1997, 2002; Coffin et al., 2002; Srivastava and Sinha, 2004a, 2004b; Ghatak and Basu, 2011; Srivastava et al., 2014; and references therein), where most Cretaceous magmatism is considered to have been part of the Greater Kerguelen large igneous province (cf. Olierook et al., 2017). Both the Deccan and Greater Kerguelen large igneous provinces include alkaline (both sodic and potassic)–ultramafic–carbonatite complexes and mafic dikes (cf. Srivastava, 1994, 1997, 2019; Simonetti et al., 1998; Karkare and Srivastava, 1990; Kent et al., 2002; Srivastava and Sinha, 2004a, 2004b, 2007; Srivastava et al., 2005, 2008a, 2008b, 2009, 2014, 2019b; Chalapathi Rao and Lehmann, 2011; Ghatak and Basu, 2013; Chalapathi Rao et al., 2011, 2014; Ernst, 2014).

More importantly in the context of the present study, Srivastava et al. (2014) pointed out that the CGC is the only terrane in the Indian Shield that appears to have experienced magmatic activity associated with both the Kerguelen and Réunion plumes. Although most of the Cretaceous magmatism in the region is related to the Kerguelen plume (Kent et al., 2002; Srivastava et al., 2009, 2014; Ghatak and Basu, 2011, 2013; Chalapathi Rao et al., 2014; Srivastava, 2020; and references therein), Kent et al. (2002) reported an age of 65.4 ± 0.3 Ma for the prominent NNW-trending Salma dolerite dike, suggesting that it may be related to the Réunion plume. However, on the basis of paleomagnetic data, Patil and Arora (2008) questioned the reported ca. 65 Ma age of the Salma dike and suggested that it was emplaced at ca. 117 Ma, consistent with other magmatic activity of the region. Geochemistry of the Salma dike is also not consistent with a ca. 65 Ma emplacement age (Srivastava et al., 2014). Srivastava et al. (2014) suggested that further geochronological study of the Salma dike is needed to resolve the uncertainty in its emplacement age. In this study, we report the results of a geochronological and geochemical study of the Salma dike, as well as a similar study of a NE-trending dike from the same region. In addition, we examined the possible link between the two dike sets and mantle plumes and associated large igneous provinces.

GEOLOGICAL BACKGROUND

The eastern and northeastern parts of the Indian Shield consist of the Singhbhum craton and the Shilling Plateau–Mikir Hills (Fig. 1). The northern portion of the Singhbhum craton is represented by the CGC, which is separated from the Singhbhum granite complex by the Singhbhum mobile belt (Fig. 1; cf. Naqvi and Rogers, 1987; Sharma, 2009; Srivastava et al., 2009, 2012, 2014). This part of the Indian Shield also includes two alkaline provinces, the Damodar Valley and the Shillong Plateau (Fig. 1; Srivastava, 2020).

The geology of the CGC has been described and discussed in detail in several publications (Naqvi and Rogers, 1987; Mahadevan, 2002; Sharma, 2009; Ramakrishnan and Vaidyanadhan, 2010; Rekha et al., 2011; and references therein). Therefore, only a brief summary is provided here. The CGC is considered to be a cratonized mobile belt of Archean age (cf. Naqvi and Rogers, 1987; Kumar and Ahmad, 2007; Sharma, 2009; Srivastava et al., 2009, 2012). The cratonic nature of the CGC is supported by a number of ENE- to E-trending intracontinental rift/shear zones responsible for distinct magmatism in the region (Ghose and Chatterjee, 2008). In general, the CGC is dominated by foliated granitoids (dominantly granite to granodiorite, occasionally tonalite) that are intrusive into amphibolites and granulite-facies gneisses and schists and occur as mesoscopic to regional-scale enclaves. The craton includes gabbros, massif anorthosites, peraluminous granite plutons, rapakivi granites, leptynites, komatiitic and tholeiitic sills/dikes, and flood basalts that range in age between late Paleoproterozoic and Early Tertiary (cf. Chatterjee et al., 2008; Ghose and Chatterjee, 2008; Chatterjee and Ghose, 2011). Cretaceous magmatic events are also recorded (cf. Baksi, 1995; Kent et al., 1997, 2002; Chalapathi Rao et al., 2014; Srivastava et al., 2014). Sedimentary rocks of the Gondwana Supergroup were deposited during the Carboniferous (ca. 295–250 Ma; Mahadevan, 2002) and occur mainly in trough-like depressions arranged in a more or less en echelon fashion along distinct shear/fault zones. These include the NW-trending Mahanadi basin, and the E-trending Damodar Valley basins and subsidiary basins to the north and northeast of Damodar Valley (Mahadevan, 2002; Chakraborty et al., 2003).

Various magmatic rocks are associated with E-trending Proterozoic rifting in the CGC. The major lineaments linked with this extensional tectonism include the E- to ESE-trending South Purulia shear zone, roughly E-trending North Purulia shear zone, Gondwana basins along the Damodar graben (intruded by Lower Cretaceous dolerite and lamproite/orangeite dike swarms; represented by the Damodar Valley basins A to D and alkaline province in Fig. 1A), and the Narmada-Son Rift (Kent et al., 1997, 2002; Mahadevan, 2002; Ghose and Chatterjee, 2008; Ghatak and Basu, 2011; Srivastava et al., 2014; Chalapathi Rao et al., 2014). Rajmahal tholeiitic basalts (cf. Kent et al., 1997, 2002; Ghatak and Basu, 2011) and a number of mafic dikes (cf. Baksi, 1995; Kent et al., 2002; Srivastava et al., 2014) are considered to be related to the ca. 120–100 Ma Kerguelen plume.

Mafic dikes of different ages (Mesoproterozoic to Cretaceous) are well exposed in the CGC and the Damodar Valley sedimentary basins of eastern India (cf. Kent et al., 2002; Srivastava et al., 2012, 2014; see Fig. 1B). Several ENE- to E- and NNW- to NW-trending Mesoproterozoic mafic dikes intrude the basement gneisses of the CGC (Kumar and Ahmad, 2007; Srivastava et al., 2012). Cretaceous mafic dikes intrude the Damodar Valley sedimentary basins, as well as Precambrian basement rocks, and trend either NNW to NW or NNE to ENE (Kent et al., 2002; Paul, 2005; Srivastava et al., 2014). The two Cretaceous dike sets have distinct geochemical characteristics (Srivastava et al., 2014). Both sets of dikes are fresh and rarely show any hydrothermal alteration.

In this study, we focused on the dikes of the Raniganj Basin (Fig. 2). Kent et al. (2002) obtained $^{40}Ar/^{39}Ar$ ages for three Cretaceous dikes. Two of these dikes were from the Raniganj Basin and have NNW trends. One of these was interpreted to be the Salma dike, and the other was interpreted to be a separate dike parallel to the Salma dike. The third dike, also trending NNW, was from the Koderma area (see Fig. 1B). The two dikes studied by Kent et al. (2002) from the Raniganj Basin yielded quite different ages, with the one interpreted to be the Salma dike dated at 65.4 ± 0.3 Ma and the other dated at 112.5 ± 0.5 Ma. The third dike, from the Koderma area, yielded an age of 115.3 ± 0.4 Ma. There are several other NNW- to NW-trending mafic dikes exposed in the Raniganj Basin that could be related to the Salma dike (Srivastava et al., 2014). A couple of NE-trending dikes have also been reported from the Raniganj Basin (see Fig. 2).

SAMPLING AND ANALYTICAL TECHNIQUES

Sampled Dikes

Since this work aimed to settle the disagreement concerning the emplacement age of the Salma dike, a very careful sampling of dikes in the Raniganj Basin was carried out. The NNW-trending Salma dike is >50 km long, and its width varies between 40 and 100 m (Fig. 3A). It is one of the prominent geological features

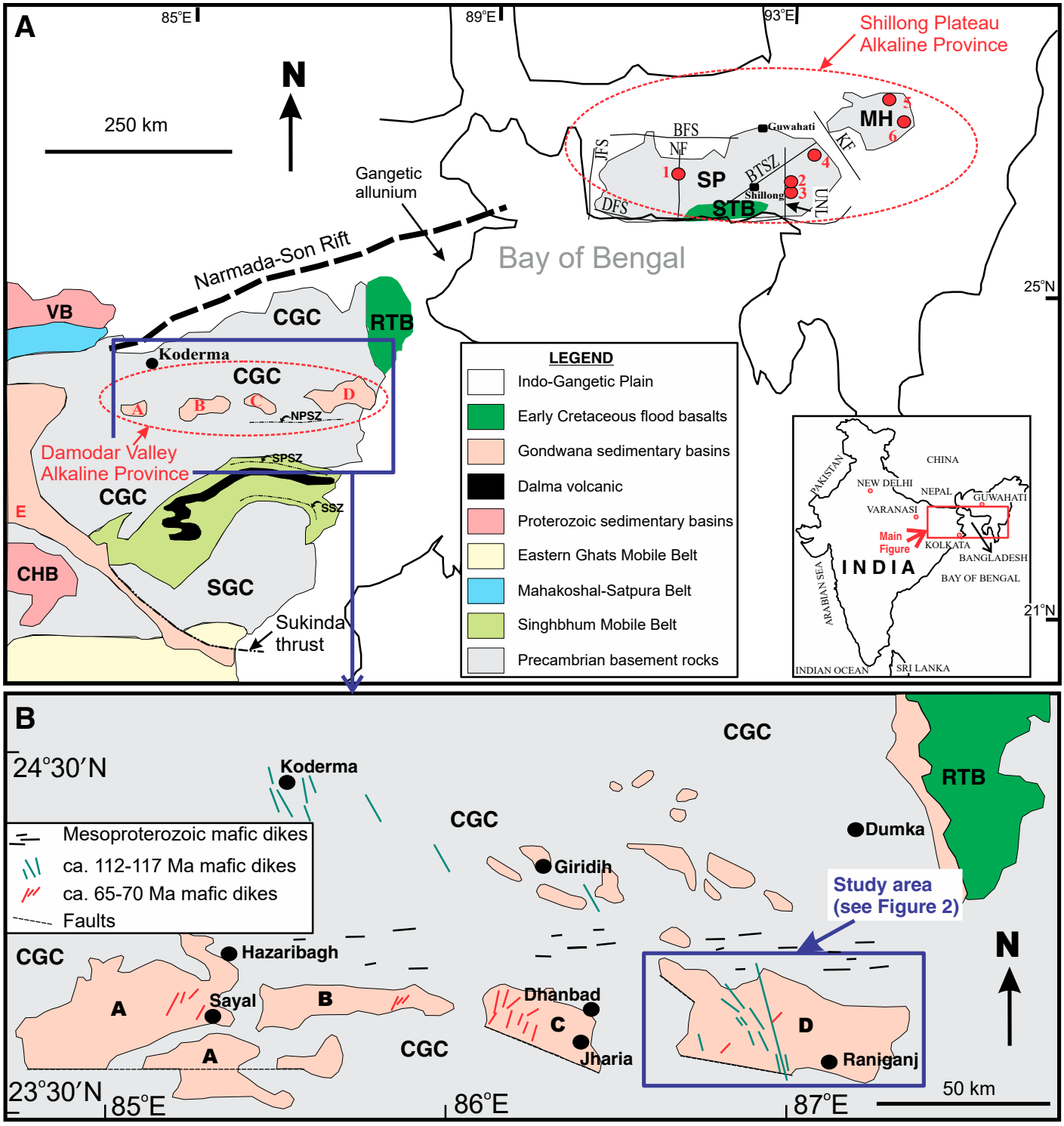

Figure 1. (A) Geological sketch map of the eastern and northeastern region of the Indian Shield showing the Singhbhum craton, consisting of Chhotanagpur gneissic complex (CGC) and Singhbhum granite complex (SGC), and the Shillong Plateau (SP)–Mikir Hills (MH) (based on and modified from Acharyya, 2003; Melluso et al., 2012; Bhowmik et al., 2012; Srivastava et al., 2019b). The Damodar Valley and Shillong Plateau alkaline provinces are also shown. (B) Distribution of Mesoproterozoic and Cretaceous mafic dikes in the CGC (modified from Kumar and Ahmad, 2007; Srivastava et al., 2014). BFS—Brahmaputra fault system; BTSZ—Badapani-Tyrsad shear zone; CHB—Chhattisgarh basin; DFS—Dauki fault system; JFS—Jamuna fault system; KF—Kopali fracture; NF—Nongcharam fault; NPSZ—North Purulia shear zone; RTB—Rajmahal tholeiitic basalt; SPSZ—South Purulia shear zone; SSZ—Singhbhum shear zone; STB—Sylhet tholeiitic basalt; UNL—Um-Ngot lineament; VB—Vindhyan Basin. A to E—Gondwana sedimentary basins (A—Karanpura; B—Bokaro; C—Jharia; D—Raniganj; E—Mahanadi). 1–6—Alkaline-carbonatite complexes in SP-MH (1—Swangkre-Rongjeng; 2—Sung Valley; 3—Mawpyut; 4—Jasra; 5—Samchampi; 6—Barpung).

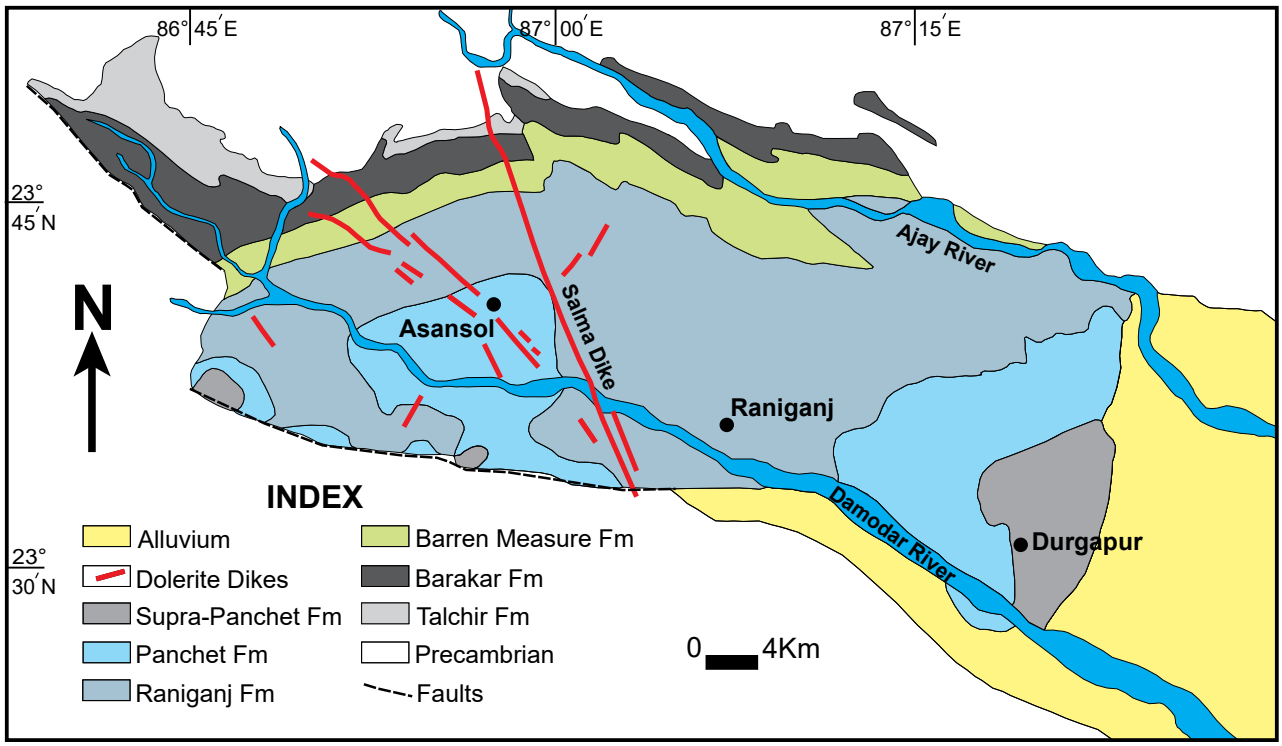

Figure 2. Geological map of the Raniganj Basin showing distribution of mafic dikes (modified after Dutta, 2003; Paul, 2005).

in the basin. Figure 3 shows locations where geochronological and geochemical samples were collected for the present study, as well as locations for the geochronological samples of the earlier study by Kent et al. (2002). The four samples in the present study were used for geochemistry, and two of these were also selected for $^{40}Ar/^{39}Ar$ dating. One dated sample (RG09/SM14) came from the Chinchuria area and definitely belongs to the Salma dike (Fig. 3C). The other (RJ13/3) is from a NE-tending dolerite dike ~600 m north of the Domohani Railway Colony, and very close to the location of the dated sample that Kent et al. (2002) interpreted to be from the Salma dike. Our NE-trending dike likely intersects the Salma dike (Fig. 3B), although the actual intersection is not exposed in the field. The mafic dike samples are coarse grained, show ophitic/subophitic textures, and consist mainly of augite/titan augite, plagioclase, and ilmenite, with a few grains of rutile and apatite.

$^{40}Ar/^{39}Ar$ Dating

In the present study, as noted above, two dolerite samples were collected from the mafic dikes of the Raniganj Basin for $^{40}Ar/^{39}Ar$ geochronological analysis. Sample RG09/SM14 came from the NNW-trending Salma dike, and sample RJ13/3 came from a NE-trending dike (see locations in Fig. 3). In order to constrain the emplacement ages and avoiding excess argon, the whole-rock fragments from the 60–80 mesh (200–280 μm in diameter) were checked carefully under a binocular microscope to remove impurities, enclaves, and phenocrysts (see Appendix for details). The final groundmass separates were dated at the Institute of Geology and Geophysics, Chinese Academy of Sciences (IGGCAS), Beijing.

Aliquots from both the samples, each containing 10 grains, were wrapped in aluminum foil to form wafers and stacked in quartz vials with the international standard YBCs (29.286 ± 0.045 Ma; Wang et al., 2014). Neutron irradiation was carried out in position H8 of the 49–2 Nuclear Reactor (49–2 NR), Beijing (China), with a flux of ~6.5×10^{12} n $(cm^2\ s)^{-1}$ for 24 h. The CO_2 laser fusion step-heating technique was used for $^{40}Ar/^{39}Ar$ analyses.

Isotopic measurements were made on the Noblesse mass spectrometer at IGGCAS. Ca and K correction factors were: $[^{36}Ar/^{37}Ar]_{Ca} = 0.000261 \pm 0.0000142$, $[^{39}Ar/^{37}Ar]_{Ca} = 0.000724 \pm 0.0000281$, $[^{40}Ar/^{39}Ar]_{K} = 0.00088 \pm 0.000023$. All argon isotopes were measured using electron multipliers in ion-counting mode. Ages were calculated using the decay constant (5.531×10^{-10} yr^{-1}) reported by Renne et al. (2011), and all errors are quoted at the 2σ level. Different decay constants (Steiger and Jäger, 1977; Min et al., 2000) were used to recalculate the data for sample RG09/SM14 in order to make a direct comparison with the previous results of Kent et al. (2002), and to check for any bias in the ages associated with the different decay constants (Table A1). The recalculation shows that the bias in ages arising from different decay constants is minor (<0.25 Ma; in other words, <0.36% for both the samples) and undetectable within errors (see Table A1; Appendix).

Plateau ages were determined from three or more contiguous steps comprising >50% of the ^{39}Ar released, revealing concordant ages at the 95% confidence level. The age errors reported here are internal errors, including analytical errors and errors on blanks, Ca and K correction factors, mass-discrimination, and *J* value; the error on the total decay constant was not propagated into the age error. Uncertainties on all data reported herein are at the 95% confidence level (2σ). The data were processed using ArArCALC (Koppers, 2002). The detailed protocol of the $^{40}Ar/^{39}Ar$ analysis technique is described in the Appendix.

Whole-Rock Geochemistry

Although geochemical data from the Cretaceous mafic dikes of the Damodar Valley (including the Salma dike) were presented in Srivastava et al. (2014), four new fresh mafic dike samples were analyzed for whole-rock

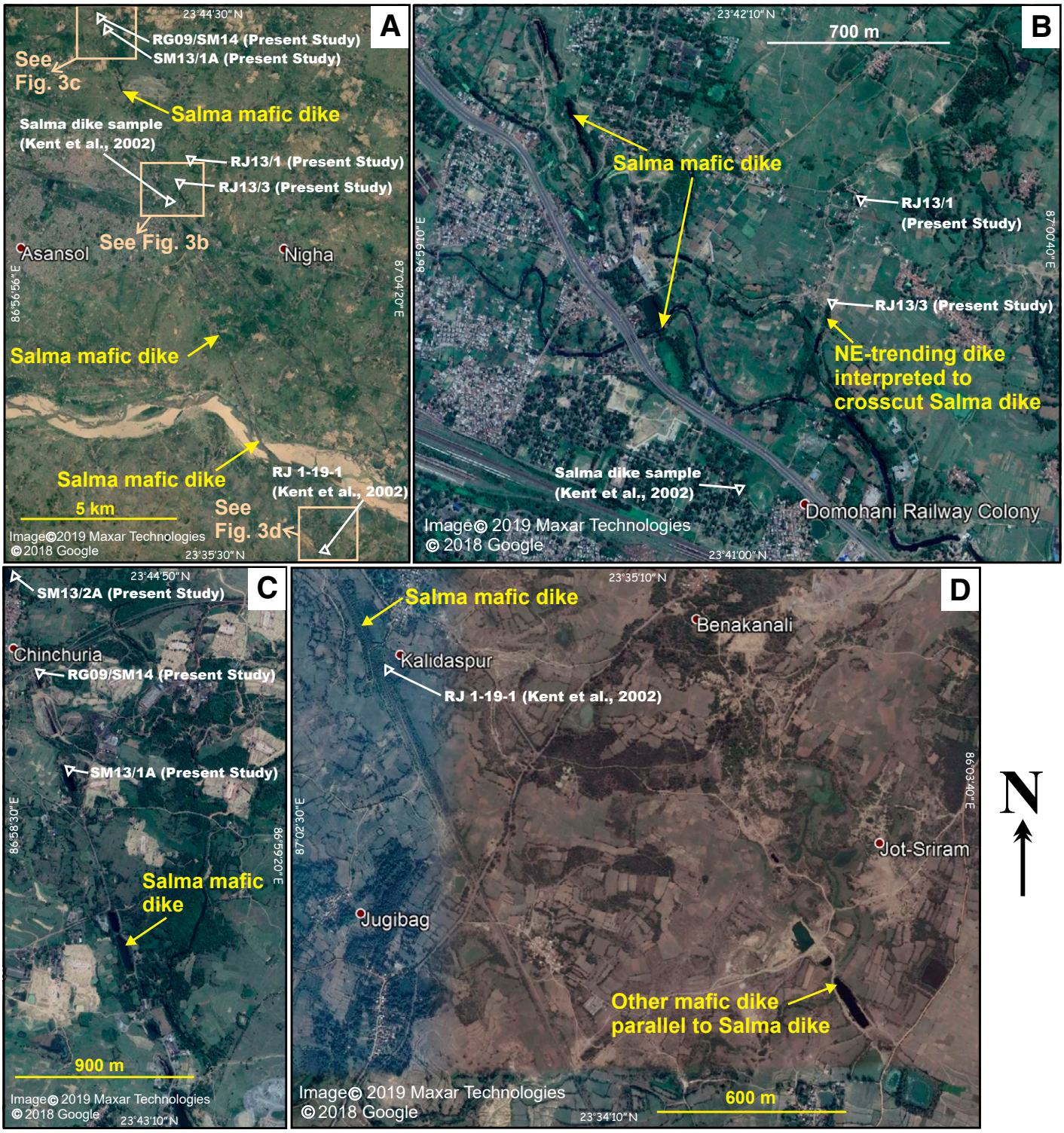

Figure 3. Google™ Earth images showing locations of the samples studied herein for ^{40}Ar-^{39}Ar geochronology and geochemistry. Dated samples (^{40}Ar-^{39}Ar method) of Kent et al. (2002) are also shown. (A) Long NNW-trending Salma dike intruded within the Raniganj Basin. (B) NE-trending mafic dike, which is interpreted to intersect the NNW Salma dike near Domohani, Asansol city. (C) Salma dike exposed near Chinchuria. (D) Salma dike and another mafic dike parallel to it near Kalidaspur. Note that Kent et al. (1997, 2002) interpreted the dike from which they collected sample RJ 1–19–1 to be a dike parallel to the Salma dike, rather than the Salma dike itself, as reinterpreted herein.

geochemistry herein, including the two samples that were later used for $^{40}Ar/Ar^{39}$ analyses (for sample locations, see Fig. 3). Geochemical data for the four freshly analyzed samples and a sample analyzed earlier by Srivastava et al. (2014) are presented in Table 1. All analyses were carried out at the Activation Laboratories, Ltd., Ancaster, Ontario, Canada. An inductively coupled plasma–optical emission spectrometer (ICP-OES; model: Thermo-JarretAsh ENVIRO II) was used to analyze major elements, whereas an inductively coupled plasma–mass spectrometer (ICP-MS; model: Perkin Elmer Sciex ELAN 6000) was used to determine trace and rare earth element (REE) concentrations. The precision was ~5% and 5%–10% for the major oxides and trace elements, respectively, when reported for concentrations at 100× detection limit. Several geostandards were run with the studied samples to check accuracy and precision. The analytical procedure was described by Gale et al. (1997), and details are available on the Activation Laboratories Ltd. website (http://www.actlabs.com).

DISCUSSION

Geochemical Characteristics

The geochemical characteristics of the Cretaceous mafic dikes exposed in Damodar Valley were comprehensively studied by Srivastava et al. (2014). They determined that the dikes trending NNE to ENE have geochemical signatures that are distinct from the dikes trending NW to NNW. The NE-trending dikes have higher concentrations of Ti, Fe, and high field strength elements (HFSEs) and are referred to as high-Ti dolerite dikes. The NW-trending dikes have comparatively lower concentrations of Ti, Fe, and HFSEs and are referred to as low-Ti dolerite dikes. It is significant that both have comparable MgO contents, despite different HFSEs values, suggesting their derivation from manifestly different mantle melts.

Geochemical data obtained for samples in the present study (Table 1) are comparable with the high-Ti dolerite and low-Ti dolerite groupings identified in the earlier geochemical study (Srivastava et al., 2014). Samples from the NE-trending mafic dike studied herein showed high concentrations of Ti, Fe, and HFSEs compared to the NNW-trending Salma dike samples. The NE dike samples fall in the basalt field on a total alkali-silica (TAS) classification diagram, whereas the NNW Salma dike samples fall in the basaltic andesite field (Fig. 4A; Irvine and Baragar, 1971; Le Maitre et al., 2002).

Geochemical distinctions between the NW- and NE-trending sets of dikes in the present study are also very evident in variation diagrams and comparable with the previously studied Cretaceous mafic dikes of this region. Two such variation plots are shown in Figures 4B and 4C. The multi-element (ME) and REE patterns of the high-Ti dolerite and low-Ti dolerite samples are also distinct (Fig. 5). The REE pattern of the NE-trending dike is comparatively more inclined (La_N/Lu_N ratios ~3.4) than the REE patterns of the NNW-trending Salma dike (La_N/Lu_N ratios ~2.4). This suggests that the high-Ti dolerite samples crystallized from a melt generated through a lower percentage melting of a mantle source than the low-Ti dolerite samples (cf. Cullers and Graf, 1984; Hirschmann et al., 1998).

The Zr/Y and Nb/Y ratios were examined to identify any involvement of a plume component in their genesis (Fig. 6A; Fitton et al., 1997; Baksi, 2000); the samples of both groups showed a possible plume connection and less likelihood of any crustal involvement. Correspondingly, the Th/Ta versus La/Ta ratio plot (Fig. 6B; cf. Kent et al., 1997; Srivastava et al., 2014) also indicates less possibility of any crustal contamination, as samples of both dike sets plot well away from the average continental crust and close to the primordial mantle value. Their geochemistry is also comparable with the geochemistry of basalts of the Kerguelen Plateau, Bunbury Island, and Rajmahal Group I (Fig. 6B; cf. Storey et al., 1992; Salters et al., 1992; Mahoney et al., 1995; Frey et al., 1996). Therefore, it appears that crustal contamination has not played a significant role in the petrogenesis of the samples studied herein.

The observed geochemical characteristics of the dike samples studied herein are consistent with those of the earlier study (cf. Srivastava et al., 2014); however, they appear to be inconsistent with the emplacement age reported by Kent

TABLE 1. WHOLE-ROCK MAJOR OXIDES (WT%) AND TRACE AND RARE EARTH ELEMENT COMPOSITIONS (IN PPM) OF THE NNW-TRENDING SALMA DIKE AND A NE-TRENDING MAFIC DIKE (INTERPRETED TO CROSSCUT THE SALMA DIKE) FROM THE RANIGANJ BASIN, DAMODAR VALLEY, EASTERN INDIA

Sample no.:	NNW Salma dike			NE mafic dike	
	SM13/1A	SM13/2A	RG09/SM14	RJ13/1	RJ13/3
SiO_2	52.33	52.51	52.70	49.69	49.62
TiO_2	1.37	1.42	1.66	3.20	3.26
Al_2O_3	15.26	15.05	14.60	12.70	12.31
Fe_2O_3	10.11	10.43	11.60	16.80	16.58
MnO	0.14	0.16	0.16	0.23	0.24
MgO	6.44	6.13	6.06	4.67	4.60
CaO	10.18	10.20	9.51	9.55	9.51
Na_2O	2.54	2.64	2.68	2.40	2.39
K_2O	0.51	0.53	0.59	0.63	0.65
P_2O_5	0.16	0.17	0.20	0.33	0.35
LOI	1.30	1.68	1.01	0.57	0.46
Total	**100.34**	**100.92**	**100.77**	**100.77**	**99.97**
Rb	9	10	10	18	18
Ba	152	228	376	171	189
Sr	296	277	279	229	227
Nb	5	5	7	15	16
Ta	0.3	0.3	0.4	1.0	1.1
Zr	85	86	95	200	206
Hf	2.2	2.4	2.8	5.0	4.9
Y	22	22	26	37	40
Th	0.9	0.7	1.1	2.1	2.3
U	0.2	0.2	0.2	0.6	0.6
La	7.90	7.40	8.70	18.5	19.8
Ce	18.50	17.30	20.50	42.80	45.4
Pr	2.64	2.49	2.60	5.98	6.38
Nd	12.30	12.30	12.40	27.70	29.10
Sm	3.60	3.90	3.90	7.40	7.90
Eu	1.38	1.44	1.38	2.30	2.38
Gd	4.20	4.30	4.70	7.80	7.80
Tb	0.70	0.80	0.80	1.30	1.40
Dy	4.50	4.60	4.70	7.70	8.10
Ho	0.90	0.90	0.90	1.50	1.50
Er	2.50	2.50	2.60	4.20	4.30
Tm	0.37	0.38	0.38	0.63	0.65
Yb	2.20	2.30	2.50	3.90	4.10
Lu	0.31	0.32	0.38	0.55	0.56

Note: LOI—loss on ignition.

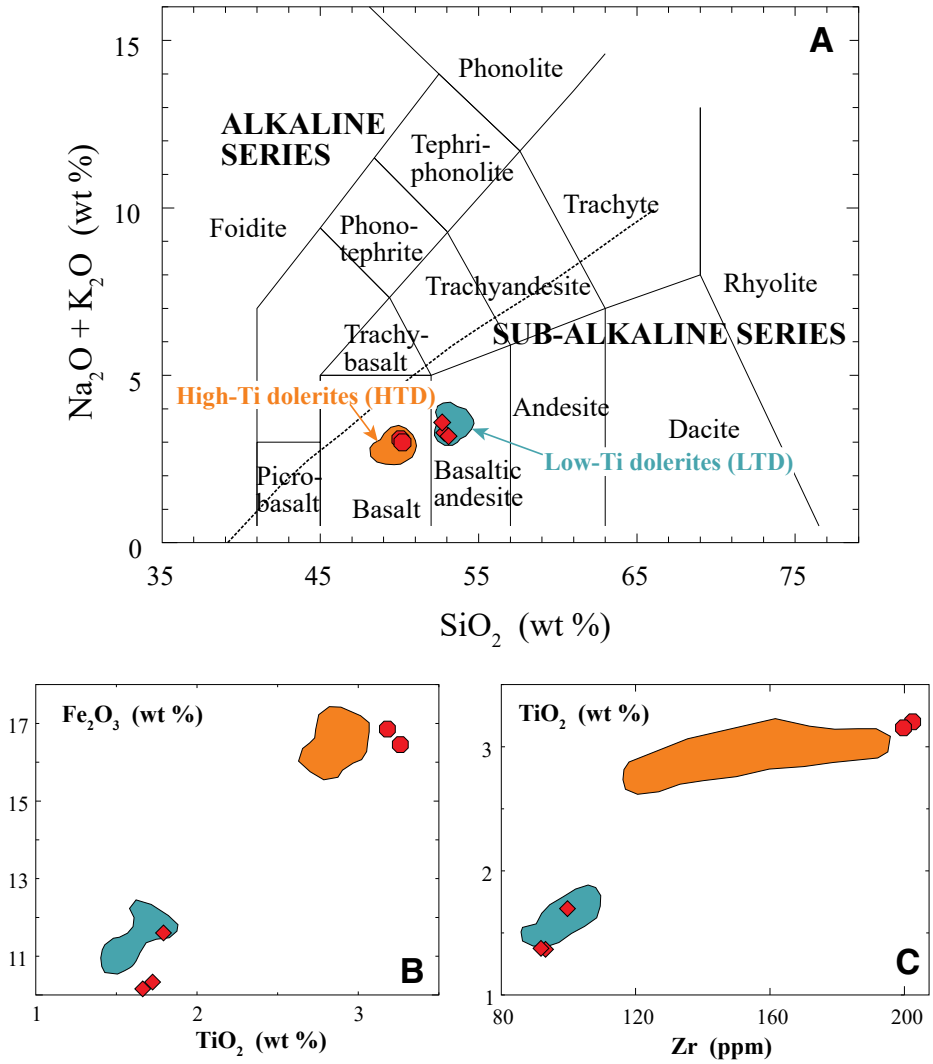

Figure 4. (A) Total alkali-silica (TAS) classification diagram (after Le Maitre et al., 2002). Dotted line discriminates between subalkaline basalts and alkaline basalts (after Irvine and Baragar 1971). (B) TiO_2 (wt%) vs. Fe_2O_3 (wt%) plot. (C) Zr (ppm) vs. TiO_2 (wt%) plot. Symbols: red circles—NE dike samples, red diamonds—NNW Salma dike samples. The fields of previously studied high-Ti dolerites (HTD; orange field) and low-Ti dolerites (LTD; sea-green field) are also shown for comparison (after Srivastava et al., 2014).

et al. (2002) for the Salma dike. In particular, the NNW-trending Salma dike, with a reported age of 65.4 ± 0.3 Ma (Kent et al., 2002), has geochemistry that is indistinguishable from that of another NNW-trending (low-Ti dolerite group) dike that was dated at 112.5 ± 0.5 (Kent et al., 2002), but quite different from the geochemistry of NE-trending (high-Ti dolerite group) dikes. The paleomagnetic pole for the Salma dike is similar to that of the ca. 117 Ma Rajmahal Traps (Patil and Arora, 2008), also suggesting that there could be a problem with the reported age of the Salma dike. To resolve this issue, we carried out $^{40}Ar/^{39}Ar$ dating for two samples, one from the Salma dike and the other from a NE-trending dike, as described in the next section.

^{40}Ar-^{39}Ar Ages

The $^{40}Ar/^{39}Ar$ data for the two geochronological samples are listed in Table 2, and age spectra and inverse isochron plots are shown in Figure 7. The sample from the NNW-trending Salma dike (RG09/SM14), collected from the Chinchuria area (Fig. 3C), yielded consistent plateau (116.0 ± 1.4 Ma) and inverse isochron (117.8 ± 2.9 Ma) ages within errors, suggesting there is no excess argon residing in the sample. This is also indicated by the trapped argon composition of 277.4 ± 25.8, which is within error of atmospheric Ar (295.5 ± 0.5). Therefore, we used the more precise age of 116.0 ± 1.4 Ma as the emplacement age of this sample. This age is quite different from the $^{40}Ar/^{39}Ar$ age of 65.4 ± 0.3 Ma for the Salma dike reported by Kent et al. (2002).

The sample from the NE-trending dike (RJ13/3) was collected ~600 m north of the Domohani Railway Colony (Fig. 3B); as noted earlier, this dike likely crosscuts the NNW-trending Salma dike, although the actual intersection is not observed. Similar to our analysis of the Salma dike data, we prefer the plateau age of 70.5 ± 0.9 Ma, rather than the inverse isochron age of 69.5 ± 3.5 Ma, as representing the time of emplacement of this dike. It is noteworthy that the age of the NE-trending dike is close to the age that was reported for the NNW-trending Salma dike by Kent et al. (2002).

Our NE-trending dike sample (RJ13/3) was collected close to the sampling site (i.e., 2 km northeast of Asansol; as mentioned in Kent et al., 1997; see Fig. 3B) that Kent et al. (2002) interpreted to be on the Salma dike and where they obtained an age of ca. 65 Ma. The similar $^{40}Ar/^{39}Ar$ ages of the NE-trending dike (sample RJ13/3) in this study and the dike of Kent et al. (2002) strongly suggest that the sample in the Kent et al. (2002) study was actually collected from the NE-trending dike (or perhaps another nearby NE-trending dike, given that there is a small difference of ~5 m.y. between the ages for the two dikes), and was not collected from the Salma dike. This interpretation is further strengthened by considering the location of another dated sample (RJ 1–19–1; ~1 km west of Kalidaspur; Fig. 3D) collected by Kent et al. (1997) from a NNW dolerite dike, which yielded a $^{40}Ar/^{39}Ar$ age of 112.5 ± 0.5 Ma (Kent et al., 2002). The location of this sample indicates that it was likely collected from the SE extension of the Salma dike (see Figs. 3A and 3D), not from another dike parallel to the Salma dike at Kalidaspur, as suggested by Kent et al. (1997).

All these observations indicate that the sample that Kent et al. (2002) dated and interpreted to be from the NNW-trending Salma dike, based on the description of Kent et al. (1997), was actually from a NE-trending dike, rather than from the Salma dike. In addition, it is clear that the correct emplacement age of the Salma dike is 116.0 ± 1.4 Ma, not 65.4 ± 0.3 Ma.

Linkage to Mantle Plume Tectonics and Large Igneous Provinces

From the new $^{40}Ar/^{39}Ar$ geochronology and geochemical data presented in this work and the discussion above, the following two broad inferences can be drawn:

(1) The NNW-trending Salma dike was emplaced at 116.0 ± 1.4 Ma and not at 65.4 ± 0.3 Ma (as suggested earlier; Kent et al., 2002).

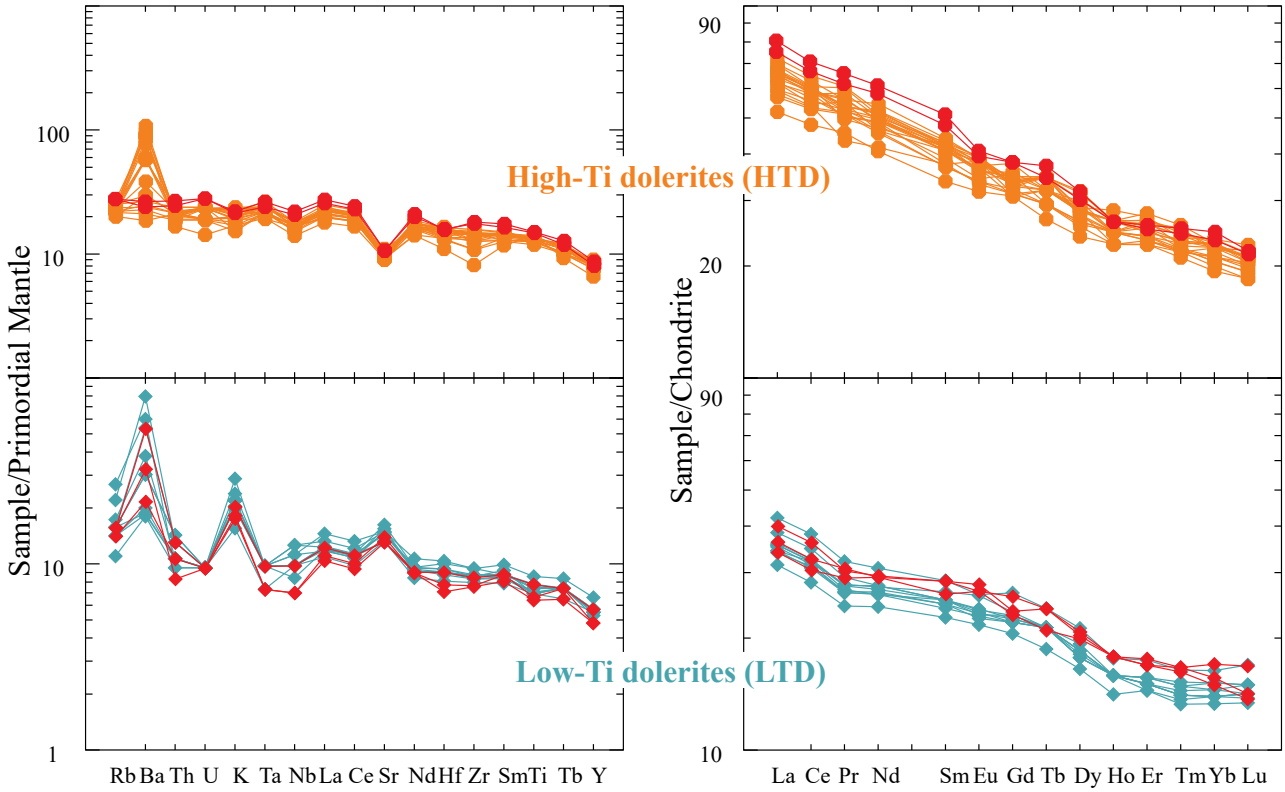

Figure 5. Primordial mantle–normalized multi-element spidergrams and chondrite-normalized rare earth element patterns for Cretaceous mafic dikes of the present study from the Raniganj Basin, as well as high-Ti dolerite and low-Ti dolerite samples. Primordial mantle and chondrite values are taken from McDonough et al. (1992) and Evensen et al. (1978). Red circles are NE dike samples and red diamonds are NNW Salma dike samples from the present study. Orange circles are high-Ti dolerites and sea-green diamonds are low-Ti dolerites from Srivastava et al. (2014).

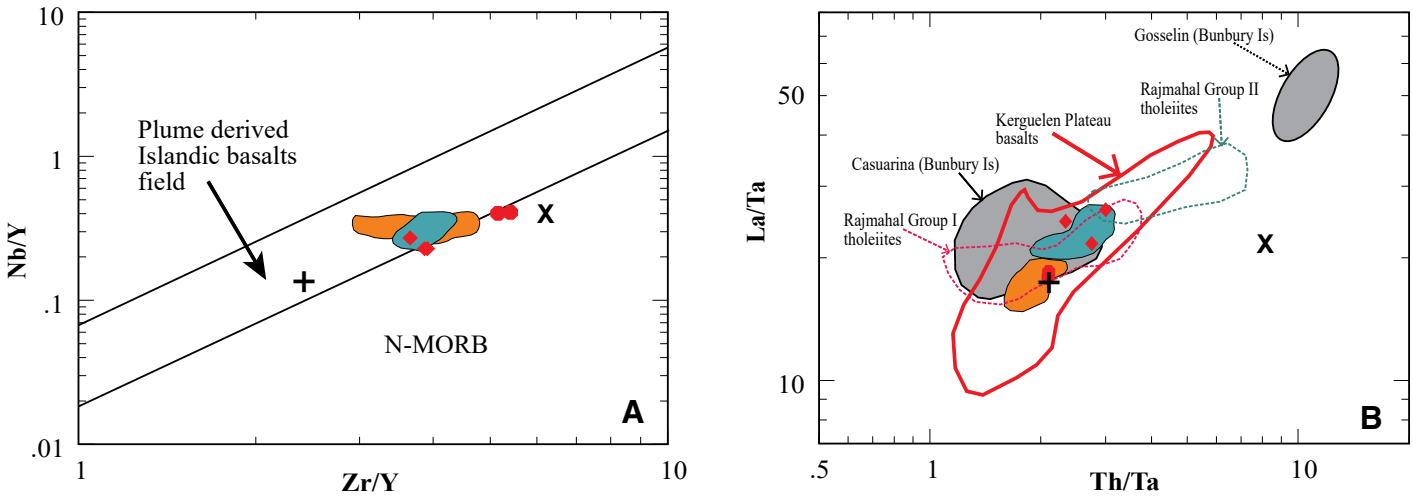

Figure 6. (A) Zr/Y vs. Nb/Y ratio plot (after Fitton et al., 1997; Baksi, 2000) for samples of present study, as well as high-Ti dolerite and low-Ti dolerite samples. (B) Th/Ta vs. La/Ta ratio plot. Fields were taken from Kent et al. (1997). Kerguelen plateau basalts—Salters et al. (1992) and Mahoney et al. (1995); Rajmahal Group I and II basalts—Storey et al. (1992); and Bunbury Island (both Gosselin and Casuarina types) basalts—Frey et al. (1996). Values of primordial mantle (+; after McDonough and Sun, 1995) and average continental crust (x; after Rudnick and Fountain, 1995) are also shown for comparison. Other symbols are the same as those in Figure 4. N-MORB—normal mid-ocean-ridge basalt.

TABLE 2. $^{40}Ar/^{39}Ar$ DATA FOR CO_2 LASER INCREMENTAL STEP-HEATING ANALYSES OF GROUNDMASS FROM RG09/SM14 AND RJ13/3

Laser (W)	$^{40}Ar/^{39}Ar$	$^{37}Ar/^{39}Ar$	$^{36}Ar/^{39}Ar$	$^{40}Ar^*/^{39}Ar_k$	$^{40}Ar^*$ (%)	$^{39}Ar_k$ (%)	Age (Ma)	±2σ
RG09/SM14, 10 grains (200–280 μm) of groundmass, J = 0.00176800 ± 0.00000884								
1.60	78.193347	1.837970	0.153750	32.95770	42.08	4.14	102.41	± 7.62
1.70	58.981221	2.534441	0.075059	37.08288	62.74	7.85	114.83	± 3.99
1.80	50.410211	2.240767	0.047391	36.65399	72.57	9.46	113.55	± 3.06
1.90	47.004864	3.211667	0.032664	37.71107	80.01	10.01	116.72	± 2.58
2.00	46.163157	3.141650	0.030071	37.62740	81.29	11.80	116.47	± 2.33
2.10	45.321229	3.416633	0.027559	37.55832	82.63	6.98	116.26	± 2.78
2.20	46.357722	3.882230	0.031720	37.41673	80.45	8.53	115.83	± 2.79
2.30	45.574203	3.687282	0.029162	37.36712	81.73	8.90	115.69	± 2.64
2.40	45.847757	3.827612	0.027918	38.02598	82.67	9.50	117.66	± 2.61
2.50	45.466290	3.974935	0.028816	37.39349	81.97	8.24	115.77	± 2.64
2.60	45.995475	3.876348	0.031470	37.12667	80.45	8.15	114.96	± 2.81
2.70	45.588829	5.093547	0.027493	38.03427	83.07	6.45	117.69	± 3.39
RJ13/3, 10 grains (200–280 μm) of groundmass, J = 0.00174500 ± 0.00000873								
1.60	33.545302	0.889842	0.057195	16.72755	49.83	7.91	52.03	± 2.70
1.70	25.278648	1.091163	0.012431	21.71216	85.81	4.79	67.25	± 1.98
1.80	24.524985	1.344282	0.007533	22.43117	91.36	4.92	69.43	± 1.82
1.90	24.443498	1.647999	0.004925	23.15151	94.58	7.61	71.62	± 1.37
2.00	24.332572	1.890822	0.004164	23.28955	95.56	8.81	72.04	± 1.35
2.10	24.077054	1.647098	0.004800	22.82144	94.65	9.94	70.62	± 1.18
2.20	23.611197	1.740384	0.004168	22.55094	95.37	11.16	69.80	± 1.16
2.30	23.632124	2.068614	0.003944	22.67084	95.76	10.40	70.16	± 1.25
2.40	23.809221	2.361335	0.005153	22.51924	94.39	10.63	69.70	± 1.18
2.50	23.700121	2.978236	0.004275	22.73114	95.67	9.12	70.34	± 1.23
2.60	23.317797	2.691358	0.004530	22.24371	95.17	8.09	68.86	± 1.32
2.70	23.360119	2.967936	0.005715	21.96245	93.78	6.62	68.01	± 1.47

(2) The eastern and northeastern Indian Shield hosts magmatic activity related to both the Kerguelen and Réunion plumes (cf. Srivastava et al., 2014), as evident from the Early Cretaceous (ca. 118–101 Ma) and Late Cretaceous (ca. 70–65 Ma) ages obtained by Kent et al. (2002) and in the present study.

The eastern and northeastern part of the Indian Shield experienced a prolonged period of magmatic activity in the Early Cretaceous (ca. 118–101 Ma; cf. Ghatak and Basu, 2011, 2013; Srivastava et al., 2019b; and references therein). Many authors interpret the magmatism to have been derived directly from melting in the Kerguelen plume head, although some recent studies, particularly those based on isotopic data, suggest an indirect relation to the plume (cf. Ghatak and Basu, 2011, 2013; Olierook et al., 2017; Srivastava et al., 2019b; and references therein), with the plume providing the heat necessary to melt the source regions (cf. Olierook et al., 2017; Srivastava et al., 2019b). The Greater Kerguelen large igneous province has been identified over a wide region in East Gondwana (cf. Olierook et al., 2017) and is thought to include the Comei Province (140–130 Ma; Zhu et al., 2009; Olierook et al., 2017), Bunbury Basalt (ca. 137–130 Ma; Olierook et al., 2016), Abor volcanics (ca. 132 Ma; Singh et al., 2019), Wallaby Plateau (ca. 124 Ma; Olierook et al., 2016), Rajmahal-Sylhet-Bengal Traps (ca. 118–112 Ma; Kent et al., 2002; Ghatak and Basu, 2011), mafic dikes recorded from the CGC (ca. 117–112 Ma; Kent et al., 2002; present study), Beaver Lake, Antarctica (ca. 117–110 Ma; Foley et al., 2002), Elan Bank (112–109 Ma; Ingle et al., 2002), and Naturaliste Plateau (>100 Ma; Pyle et al., 1995).

The younger Late Cretaceous magmatic event (70–65 Ma; Kent et al., 2002; present work) of eastern and northeastern India was likely connected to the Réunion plume and the associated Deccan large igneous province of western India (Kent et al., 2002; Paul, 2005; Srivastava et al., 2014). While it is well established that the bulk (>90%) of Deccan volcanism occurred at 65 (±1) Ma, close to the Cretaceous-Tertiary boundary (Duncan and Pyle, 1988; Baksi, 1994; Allègre et al., 1999; Hofmann et al., 2000; Chenet et al., 2007; Schoene et al., 2015, 2019; Sprain et al., 2019), more limited Deccan volcanism occurred before and after the main event between 69 and 62 Ma (Widdowson et al., 2000; Pande, 2002; Hooper et al., 2010; Chalapathi Rao and Lehmann, 2011). Volcanic rocks that are thought to be associated with the Réunion plume have also been identified far from the main Deccan large igneous province in western India. For example, Mahoney et al. (2002) obtained a 72 Ma age for Réunion hotspot–related lavas in the South Tethyan suture zone of Pakistan that have very similar isotopic and trace-element geochemistry to the Deccan large igneous province (Mahoney, 1988). In addition, 64.7 ± 0.5 Ma Rajahmundry lavas along India's eastern coast, >400 km from the main Deccan lavas, are thought to have been part of the Deccan event (Knight et al., 2003). It appears likely that the huge (2000–2500-km-diameter) Réunion mantle plume head and/or heat associated with it was responsible for all these volcanic eruptions, as well as for continental breakup of greater India with the Seychelles (cf. White and McKenzie, 1989; Mahoney et al., 2002).

Overall, the new $^{40}Ar/^{39}Ar$ ages obtained from the two geochemically distinct sets of doleritic dikes in the CGC of eastern India indicate that they were intruded in extensional tectonic settings associated with the Kerguelen and Réunion mantle plumes. However, in both the cases, the plume was likely not directly involved, but rather provided additional heat necessary to melt the mantle source. More robust geochronological, radiogenic isotope geochemical, and paleomagnetic data are required to determine the overall extent of these two events and better constrain the relative contributions of the plumes to their genesis.

CONCLUSIONS

The NNE to ENE and NW to NNW Cretaceous mafic dikes exposed in the Chhotanagpur gneissic complex of eastern India show very distinct geochemical characteristics and are identified as high-Ti and low-Ti dolerites, respectively. In the Raniganj Basin, dikes of these two sets were dated by the $^{40}Ar/^{39}Ar$ method to resolve a controversy concerning the emplacement age of the long NNW-trending Salma dike.

The NE-trending dike has a $^{40}Ar/^{39}Ar$ plateau age of 70.5 ± 0.9 Ma, whereas the NNW-trending Salma dike has a plateau age of 116.0 ± 1.4 Ma, indicating that the Salma dike was emplaced at ca. 116 Ma, not at ca. 65 Ma as suggested previously.

The genesis of the two dike sets is thought to be from melts generated during extensional tectonic regimes developed by sizeable mantle plume heads, with the plume heads providing the additional heat necessary to melt the mantle source.

The ca. 116 Ma Salma dike is interpreted as part of the Greater Kerguelen large igneous province associated with the Kerguelen mantle plume, whereas the younger ca. 70 Ma mafic dike likely belongs to the Deccan large igneous province linked to the Réunion plume.

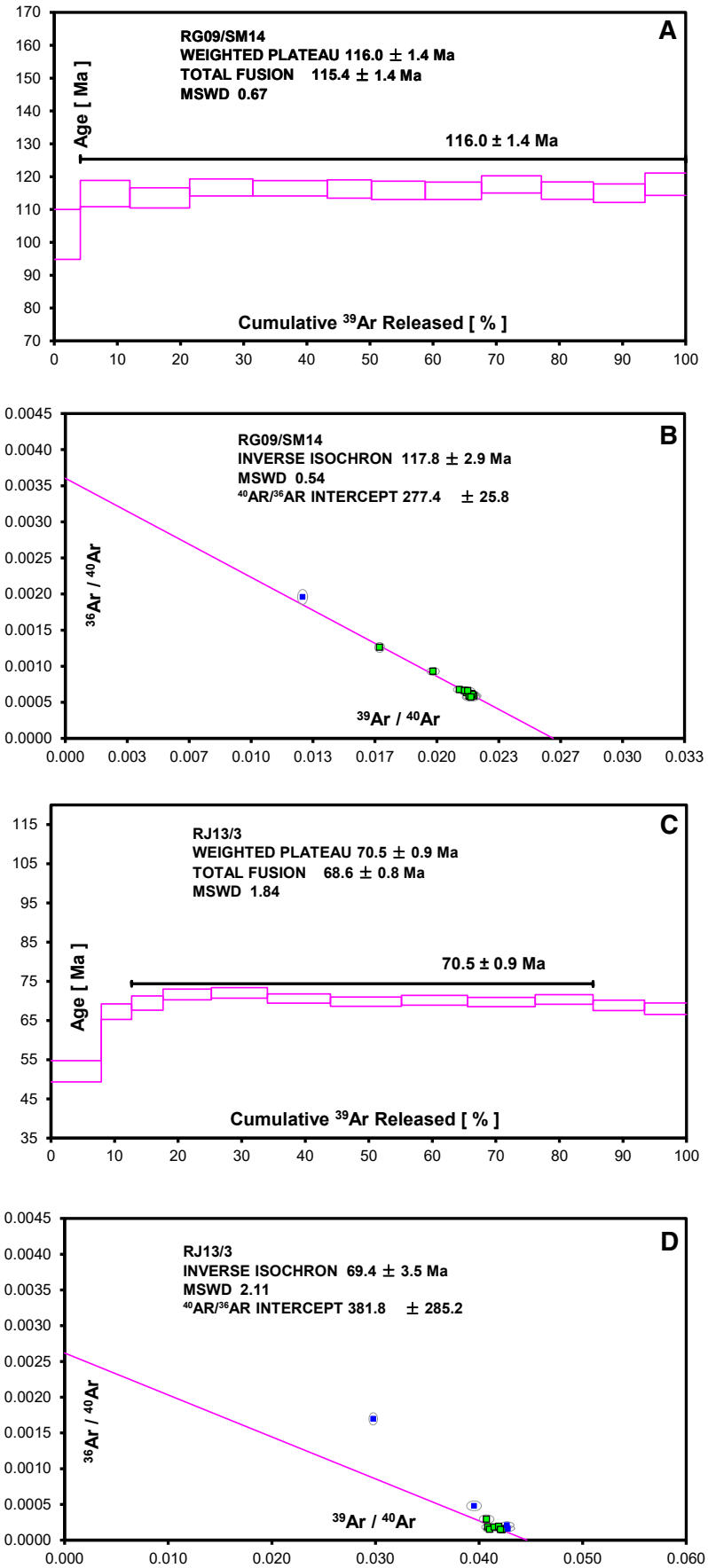

Figure 7. $^{40}Ar/^{39}Ar$ age spectra for RG09/SM14 (NNW-trending Salma dike) and RJ13/3 (NE-trending dike). Both plateau (A, C) and inverse isochron (B, D) ages are shown. In inverse isochron plots, green squares show plateau data points, and blue squares represent nonplateau data points. MSWD—mean square of weighted deviates.

ACKNOWLEDGMENTS

Srivastava thanks the Science and Engineering Research Board (SERB) for financial support through a research project (no. EMR/2016/000169), and the head of the Department of Geology, Banaras Hindu University, for extending all necessary facilities required during this work. We thank Dawn Kellett, an anonymous reviewer, and Science Editor Laurent Godin for their constructive comments that helped to improve the manuscript.

APPENDIX: DETAILED ANALYTICAL TECHNIQUES

Sample Preparation and Irradiation

The groundmass of a volcanic rock is usually quenched from melt at or near the surface during eruption. Therefore, it is a proxy for the time of eruption, and its initial argon composition is similar to that of the atmosphere (avoiding contamination from deep excess argon). In contrast, phenocrysts, such as plagioclase, may crystallize in a magma chamber in the lower crust or mantle sometime prior to its emplacement, and, hence, may trap deep argon that is different from the atmosphere (excess argon). Therefore, to constrain the emplacement age and avoid excess argon, the groundmass portions of the dolerite samples were analyzed in this study.

The samples were crushed in a steel jaw crusher followed by grinding in a steel mill. Grinding was accomplished in 1–2 second steps and alternated with sieving at 200 µm until 90% of the rock powder was reduced to <200 µm. The remaining 200–280 µm fraction included the hardest components of the altered samples and is assumed to be the freshest parts of the samples. The groundmass aliquots were then handpicked under a binocular microscope from this 200–280 µm fraction. The aliquots of every groundmass sample were inspected carefully to remove phenocrysts or xenocrysts, and all other impurities.

The separates of groundmass were further cleaned by acid-leaching with 2 *N* HNO_3 for 30 min in an ultrasonic bath and heated to 50 °C in order to remove the calcite and other nitric-soluble phases. The leached separates were washed in an ultrasonic bath in deionized water three times, each for 30 min, and then in acetone three times (for 30 min), and dried in preparation for irradiation.

All sample aliquots were wrapped in aluminum foil to form wafers and stacked in quartz vials with the international standard YBCs. The vials were 40 mm in length, with an inner diameter of 6.5 mm. The position for each sample was recorded as the distance from the bottom of the vial. Then, the vials were sealed in vacuo and put in a quartz canister. The canister was wrapped with cadmium foil (0.5 mm in thickness) for shielding slow neutrons in order to prevent interface reactions during the irradiation.

Neutron irradiation was carried out in position H8 of 49–2 Nuclear Reactor (49–2 NR), Beijing (China), with a flux of ~6.5 × 10^{12} n (cm^2 $s)^{-1}$ for 24 h, yielding *J* values of ~0.0017. The H8 position lies in the core of the reactor and receives flux from all directions. Specimens were rotated during the fast neutron irradiation to get homogeneously distributed neutrons. Six to eight replicate analyses of the monitors from each vial were conducted to constrain the vertical neutron fluence gradient to within ±0.7%. This additional uncertainty was propagated into the plateau and inverse isochron ages. External uncertainties arising from the decay constants and primary K-Ar standards were not propagated. Errors are reported at the 2σ confidence level.

Gas Extraction and Mass Spectrometry Analyses

Argon isotope analyses were carried out on a mass-spectrometry system at the $^{40}Ar/^{39}Ar$ geochronology laboratory at

the Institute of Geology and Geophysics, Chinese Academy of Sciences (IGGCAS), Beijing, China. The system, a product of NU Instrumental Company based in the UK, consists of a CO_2 laser (50 W, 10.6μm wavelength, 999 Hz), a gas purification preparation line, and a Noblesse mass spectrometer.

The irradiated samples were moved into 2-mm-diameter wells in a copper sample holder, which was then placed in a ZnSe windowed chamber. After preheating under pumping at 140 °C for 72 h by using heating tapes, the samples were heated in stepwise fashion to extract gas by using a continuous 2-mm-spot CO_2 laser beam. Twelve heating steps, each for 3 min, were performed for each sample with laser outputs from 1.6 to 2.7 W at steps of 0.1 W until the samples were completely molten (the grains turned into a black ball that did not glitter any longer under lasing). Each gas fraction was purified simultaneously during the 3 minutes using two SAES NP10 Zr-Al getters built in the prep-line, one of which ran at 400 °C to remove active gases (e.g., N_2, CO, CO_2), and the other one of which was kept at room temperature to absorb H_2. After purification, the valve between the prep-line and the mass spectrometer was switched on, and the gas was introduced into the mass spectrometer for argon isotope analyses. The entire volume of gas in the laser chamber, prep-line, and mass spectrometer was ionized and analyzed. The purity of gas and a low level of residual active gases in the mass spectrometer were maintained by another two Zr-Al getters at room temperature. Argon isotopes were measured in the order of ^{40}Ar, ^{39}Ar, ^{38}Ar, ^{37}Ar, and ^{36}Ar, and involved 13 cycles of replicate measurements. For each peak and baseline measurement, the ion beam of ^{40}Ar, ^{39}Ar, ^{38}Ar, ^{37}Ar, and ^{36}Ar was integrated for 5, 10, 5, 5, and 20 s, respectively, with baselines for 5 s. Baseline measurements were taken at a half mass unit away from the peaks, except between ^{39}Ar and ^{40}Ar, where the baseline was set at 39.3. The final measurement for each isotope was extrapolated to zero time using the least-square regression from the 13 cycle measurements. Usually the "memory effect" of the instrument was negligible; the variation of $^{40}Ar/^{39}Ar$ was less than 1% in one run, and the analytic error was less than 0.1%.

The Noblesse mass spectrometer at IGGCAS is configured as a multicollector with a high-mass Faraday cup with a 10^{11} Ω resistor and three discrete dynode secondary electron multipliers performing in ion-counting mode. Due to its well-focused ion beam and wide collector-slit spacing, the Noblesse mass spectrometer yields steep-margined and flat-topped broad peaks, with a peak flatness of ≤1 part in 10^3 over ±300 ppm on the Faraday cup and ≤2 parts in 10^3 over ±150 ppm on multipliers (without retardation filter). Electrostatic filters are positioned at the entrance of the multipliers to suppress stray ions. Interferences produced by HCl and hydrocarbon species overlap the high-mass side of all argon peaks. Argon isotopic measurements were obtained on the unaffected low-mass sides of the peaks to obtain ^{36}Ar measurements that were free of interference species (Saxton, 2015). Static backgrounds of the IGGCAS Noblesse are typically ~4.5×10^{-17}, 1.3×10^{-18}, 3.5×10^{-19}, 5.7×10^{-18}, and 4.2×10^{-19} mol for ^{40}Ar through ^{36}Ar. Procedural blanks (i.e., simulated analyses without sample gas) are ~3.8×10^{-16}, 2.0×10^{-18}, 5.1×10^{-19}, 5.5×10^{-18}, and 1.9×10^{-18} mol for ^{40}Ar through ^{36}Ar, respectively. Blanks were monitored every two measurements for correction. The efficiency (gain) of multipliers against the Faraday cup, which depends on amount of gas and is governed by "dead time" of the multiplier, is monitored every month. Mass discrimination was monitored using an online air pipette from which multiple measurements were made before and after each experiment. The mean over this period was 1.00100 ± 0.00021 per amu, and the uncertainty of this value was propagated into all age calculations.

Ages were calculated using the decay constant of Renne et al. (2011), and all errors are quoted at the 2σ level. In order to make our results comparable directly with the previous study (Kent et al., 2002) on the same dike sets, the age results for RG09/SM14 were recalculated (Table A1) using the different decay constants reported by Steiger and Jäger (1977) and Min et al. (2000). The results show that the bias in ages caused by the different decay constants is minor (<0.25 Ma; Table A1) and is undetectable within errors (Table A1).

TABLE A1. RECALCULATION OF DATA FOR SAMPLE RG09/SM14 USING DIFFERENT DECAY CONSTANTS REPORTED BY STEIGER AND JÄGER (1977) AND MIN ET AL. (2000)

Laser (W)	$^{40}Ar/^{39}Ar$	$^{37}Ar/^{39}Ar$	$^{36}Ar/^{39}Ar$	$^{40}Ar^*/^{39}Ar_k$	$^{40}Ar^*$ (%)	$^{39}Ar_k$ (%)	Age (Ma)	±2σ
$\lambda_{total} = 5.543 \times 10^{-10}$ yr^{-1} (Steiger and Jäger, 1977)								
1.60	78.193347	1.837970	0.153750	32.95770	42.08	4.14	102.18	± 7.62
1.70	58.981221	2.534441	0.075059	37.08288	62.74	7.85	114.57	± 3.99
1.80	50.410211	2.240767	0.047391	36.65399	72.57	9.46	113.29	± 3.06
1.90	47.004864	3.211667	0.032664	37.71107	80.01	10.01	116.45	± 2.58
2.00	46.163157	3.141650	0.030071	37.62740	81.29	11.80	116.20	± 2.33
2.10	45.321229	3.416633	0.027559	37.55832	82.63	6.98	115.99	± 2.78
2.20	46.357722	3.882230	0.031720	37.41673	80.45	8.53	115.57	± 2.79
2.30	45.574203	3.687282	0.029162	37.36712	81.73	8.90	115.42	± 2.64
2.40	45.847757	3.827612	0.027918	38.02598	82.67	9.50	117.39	± 2.61
2.50	45.466290	3.974935	0.028816	37.39349	81.97	8.24	115.50	± 2.64
2.60	45.995475	3.876348	0.031470	37.12667	80.45	8.15	114.70	± 2.81
2.70	45.588829	5.093547	0.027493	38.03427	83.07	6.45	117.42	± 3.39
$\lambda_{total} = 5.541 \times 10^{-10}$ yr^{-1} (Min et al., 2000)								
1.60	78.193347	1.837970	0.153750	32.95770	42.08	4.14	102.21	± 7.62
1.70	58.981221	2.534441	0.075059	37.08288	62.74	7.85	114.61	± 3.99
1.80	50.410211	2.240767	0.047391	36.65399	72.57	9.46	113.33	± 3.06
1.90	47.004864	3.211667	0.032664	37.71107	80.01	10.01	116.49	± 2.58
2.00	46.163157	3.141650	0.030071	37.62740	81.29	11.80	116.24	± 2.33
2.10	45.321229	3.416633	0.027559	37.55832	82.63	6.98	116.03	± 2.78
2.20	46.357722	3.882230	0.031720	37.41673	80.45	8.53	115.61	± 2.79
2.30	45.574203	3.687282	0.029162	37.36712	81.73	8.90	115.46	± 2.64
2.40	45.847757	3.827612	0.027918	38.02598	82.67	9.50	117.43	± 2.61
2.50	45.466290	3.974935	0.028816	37.39349	81.97	8.24	115.54	± 2.64
2.60	45.995475	3.876348	0.031470	37.12667	80.45	8.15	114.74	± 2.81
2.70	45.588829	5.093547	0.027493	38.03427	83.07	6.45	117.46	± 3.39

REFERENCES CITED

Acharyya, S.K., 2003, The nature of Mesoproterozoic central Indian tectonic zone with exhumed and reworked older granulites: Gondwana Research, v. 6, p. 197–214, https://doi.org/10.1016/S1342-937X(05)70970-9.

Allègre, C.J., Birck, J.L., Capmas, F., and Courtillot, V., 1999, Age of the Deccan Traps using ^{187}Re-^{187}Os systematics: Earth and Planetary Science Letters, v. 170, p. 197–204, https://doi.org/10.1016/S0012-821X(99)00110-7.

Baksi, A.K., 1994, Intracanyon flows in the Deccan province, India? Case history of the Rajahmundry Traps: Geology, v. 22, p. 605–608, https://doi.org/10.1130/0091-7613(1994)022<0605:IFITDP>2.3.CO;2.

Baksi, A.K., 1995, Petrogenesis and timing of volcanism in the Rajmahal flood basalt province, northeastern India: Chemical Geology, v. 121, p. 73–90, https://doi.org/10.1016/0009-2541(94)00124-Q.

Baksi, A.K., 2000, Search for a deep-mantle component in mafic lavas using Nb-Y-Zr plot: Canadian Journal of Earth Sciences, v. 38, p. 813–824.

Bhowmik, S.K., Wilde, S.A., Bhandari, A., Pal, T., and Pant, N.C., 2012, Growth of the Greater Indian landmass and its assembly in Rodinia: Geochronological evidence from the Central Indian tectonic zone: Gondwana Research, v. 22, p. 54–72, https://doi.org/10.1016/j.gr.2011.09.008.

Bleeker, W., 2003, The late Archean record: A puzzle in ca. 35 pieces: Lithos, v. 71, p. 99–134, https://doi.org/10.1016/j.lithos.2003.07.003.

Bleeker, W., 2004, Taking the pulse of planet Earth: Geoscience Canada, v. 31, p. 179–190.

Bleeker, W., and Ernst, R.E., 2006, Short-lived mantle generated magmatic events and their dike swarms: The key unlocking Earth's paleogeographic record back to 2.6 Ga, *in* Hanski, E., Mertanen, S., Rämö, T., and Vuollo, J., eds., Dike Swarms—Time Markers of Crustal Evolution: London, Taylor and Francis Group, p. 3–26, https://doi.org/10.1201/NOE0415398992.ch1.

Chakraborty, C., Mandal, N., and Ghosh, S.K., 2003, Kinematics of the Gondwana basins of peninsular India: Tectonophysics, v. 377, p. 299–324, https://doi.org/10.1016/j.tecto.2003.09.011.

Chalapathi Rao, N.V., and Lehmann, B., 2011, Kimberlites, flood basalts and mantle plumes: New insights from the Deccan large igneous province: Earth-Science Reviews, v. 107, p. 315–324, https://doi.org/10.1016/j.earscirev.2011.04.003.

Chalapathi Rao, N.V., Burgess, R., Lehmann, B., Mainkar, D., Pande, S.K., Hari, K.R., and Bodhankar, N., 2011, $^{40}Ar/^{39}Ar$ ages of mafic dykes from the Mesoproterozoic Chhattisgarh basin, Bastar craton, central India: Implication for the origin and spatial extent of the Deccan large igneous province: Lithos, v. 125, p. 994–1005, https://doi.org/10.1016/j.lithos.2011.06.001.

Chalapathi Rao, N.V., Srivastava, R.K., Sinha, A.K., and Ravikant, V., 2014, Petrogenesis of Kerguelen mantle plume–linked Early Cretaceous ultrapotassic intrusive rocks from the Gondwana sedimentary basins, Damodar Valley, eastern India: Earth-Science Reviews, v. 136, p. 96–120, https://doi.org/10.1016/j.earscirev.2014.05.012.

Chatterjee, N., and Ghose, N.C., 2011, Extensive early Neoproterozoic high-grade metamorphism in North Chotanagpur gneissic complex of the Central Indian tectonic zone: Gondwana Research, v. 20, p. 362–379, https://doi.org/10.1016/j.gr.2010.12.003.

Chatterjee, N., Crowley, J.L., and Ghose, N.C., 2008, Geochronology of the 1.55 Ga Bengal anorthosite and Grenvillian metamorphism in the Chotanagpur gneissic complex, eastern India: Precambrian Research, v. 161, p. 303–316, https://doi.org/10.1016/j.precamres.2007.09.005.

Chenet, A.L., Quidelleur, X., Fluteau, F., and Courtillot, V., 2007, ^{40}K-^{39}Ar dating of the main Deccan large igneous province: Further evidence of KTB age and short duration: Earth and Planetary Science Letters, v. 263, p. 1–15, https://doi.org/10.1016/j.epsl.2007.07.011.

Coffin, M.F., Pringle, M.S., Duncan, R.A., Gladezenko, T.P., Storey, M., Müller, R.D., and Gahagan, L.A., 2002, Kerguelen hotspot magma output since 130 Ma: Journal of Petrology, v. 43, p. 1121–1137, https://doi.org/10.1093/petrology/43.7.1121.

Courtillot, V., Féraud, G., Maluski, H., Vandamme, D., Moreau, M.G., and Besse, J., 1988, Deccan flood basalts and the Cretaceous/Tertiary boundary: Nature, v. 333, p. 843–846, https://doi.org/10.1038/333843a0.

Cullers, R.L., and Graf, J.L., 1984, Rare earth elements in igneous rocks of the continental crust: Predominantly basic and ultrabasic rocks, *in* Henderson, P., ed., Rare Earth Element Geochemistry: Amsterdam, Netherlands, Elsevier, p. 237–274, https://doi.org/10.1016/B978-0-444-42148-7.50012-5.

Curray, I.R., and Munasinghe, T., 1991, Origin of the Raj Mahal traps and the 85°E ridge preliminary reconstructions of the trace of the Crozet hotspot: Geology, v. 19, p. 1237–1240, https://doi.org/10.1130/0091-7613(1991)019<1237:OOTRTA>2.3.CO;2.

Duncan, R.A., and Pyle, D.G., 1988, Rapid eruption of the Deccan flood basalts at the Cretaceous/Tertiary boundary: Nature, v. 333, p. 841–843, https://doi.org/10.1038/333841a0.

Dutta, A.B., 2003, Coal Resources of West Bengal: Bulletin of the Geological Survey of India Series A5, 45 p.

Ernst, R.E., 2014, Large Igneous Provinces: Cambridge, UK, Cambridge University Press, 653 p., https://doi.org/10.1017/CBO9781139025300.

Ernst, R.E., and Buchan, K.L., 2001a, The use of mafic dike swarms in identifying and locating mantle plumes, *in* Ernst, R.E., and Buchan, K.L., eds., Mantle Plumes: Their Identification Through Time: Geological Society of America Special Paper 352, p. 247–265, https://doi.org/10.1130/0-8137-2352-3.247.

Ernst, R.E., and Buchan, K.L., 2001b, Large mafic magmatic events through time and links to mantle-plume heads, *in* Ernst, R.E., and Buchan, K.L., eds., Mantle Plumes: Their Identification Through Time: Geological Society of America Special Paper 352, p. 483–566. https://doi.org/10.1130/0-8137-2352-3.483.

Ernst, R., Srivastava, R.K., Bleeker, W., and Hamilton, M.A., 2010, Preface: Precambrian large igneous provinces (LIPs) and their dike swarms: New insights from high-precision geochronology integrated with paleomagnetism and geochemistry: Precambrian Research, v. 183, p. vii–xi, https://doi.org/10.1016/j.precamres.2010.09.001.

Evensen, N.M., Hamilton, P.J., and O'Nion, R.K., 1978, Rare earth abundances in chondritic meteorites: Geochimica et Cosmochimica Acta, v. 42, p. 1199–1212, https://doi.org/10.1016/0016-7037(78)90114-X.

Fitton, J.G., Saunders, A.D., Norry, M.J., Hardarson, B.S., and Taylor, R.N., 1997, Thermal and chemical structure of the Iceland plume: Earth and Planetary Science Letters, v. 153, p. 197–208, https://doi.org/10.1016/S0012-821X(97)00170-2.

Foley, S.F., Andronikov, A.V., and Melzer, S., 2002, Petrology of ultramafic lamprophyres from the Beaver Lake area of eastern Antarctica and their relation to the breakup of Gondwanaland: Mineralogy and Petrology, v. 74, p. 361–384, https://doi.org/10.1007/s007100200011.

Frey, F.A., McNaughton, N.J., Nelson, D.R., deLaeter, J.R., and Duncan, R.A., 1996, Petrogenesis of Bunbury basalts, western Australia: Interaction between the Kerguelen plume and Gondwana lithosphere?: Earth and Planetary Science Letters, v. 144, p. 163–183, https://doi.org/10.1016/0012-821X(96)00150-1.

Gale, G.H., Dabek, L.B., and Fedikow, M.A.F., 1997, The application of rare earth element analyses in the exploration for volcanogenic massive sulphide type deposits: Exploration and Mining Geology, v. 6, p. 233–252.

Ghatak, A., and Basu, A.R., 2011, The Sylhet Traps: Vestiges of the Kerguelen plume in NE India: Earth and Planetary Science Letters, v. 308, p. 52–64, https://doi.org/10.1016/j.epsl.2011.05.023.

Ghatak, A., and Basu, A.R., 2013, Isotopic and trace element geochemistry of alkalic–mafic–ultramafic–carbonatitic complexes and flood basalts in NE India: Origin in a heterogeneous Kerguelen plume: Geochimica et Cosmochimica Acta, v. 115, p. 46–72, https://doi.org/10.1016/j.gca.2013.04.004.

Ghose, N.C., and Chatterjee, N., 2008, Petrology, tectonic setting and source of dikes and related magmatic bodies in Chotanagpur gneissic complex, eastern India, *in* Srivastava, R.K., Sivaji, Ch., and Chalapathi Rao, N.V., eds., Indian Dikes: Geochemistry, Geophysics and Geochronology: New Delhi, India, Narosa Publishing House Pvt Ltd., p. 471–493.

Hirschmann, M.M., Ghiorso, M.S., Wasylenki, L.E., Asimow, P.D., and Stolper, E.M., 1998, Calculation of peridotite partial melting from thermodynamic models of minerals and melts. I. Method and composition to experiments: Journal of Petrology, v. 39, p. 1091–1115, https://doi.org/10.1093/petroj/39.6.1091.

Hofmann, C., Féraud, G., and Courtillot, V., 2000, $^{40}Ar/^{39}Ar$ dating of mineral separates and whole rocks from the Western Ghats lava pile: Further constraints on duration and age of the Deccan Traps: Earth and Planetary Science Letters, v. 180, p. 13–27, https://doi.org/10.1016/S0012-821X(00)00159-X.

Hooper, P.R., Widdowson, M., and Kelley, S.P., 2010, Tectonic setting and timing of the final Deccan flood basalt eruptions: Geology, v. 38, p. 839–842, https://doi.org/10.1130/G31072.1.

Ingle, S., Weis, D., and Frey, F.A., 2002, Indian continental crust recovered from Elan Bank, Kerguelen Plateau (ODP Leg 183, Site 1137): Journal of Petrology, v. 43, p. 1241–1257, https://doi.org/10.1093/petrology/43.7.1241.

Irvine, T.N., and Baragar, W.R.A., 1971, A guide to chemical classification of the common volcanic rocks: Canadian Journal of Earth Sciences, v. 8, p. 523–548, https://doi.org/10.1139/e71-055.

Karkare, S.G., and Srivastava, R.K., 1990, Regional dike swarms related to the Deccan Trap alkaline province, India, *in* Parker, A.J., Rickwood, P.C., and Tucker, D.H., eds., Mafic Dikes and Emplacement Mechanism: Rotterdam, Netherlands, Balkema, p. 335–347.

Kent, R.W., Saunders, A.D., Kempton, P.D., and Ghose, N.C., 1997, Rajmahal basalts, eastern India: Mantle source and melt distribution at a volcanic rifted margin, *in* Mahoney, J.J., and Coffin, M.F., eds., Large Igneous Provinces—Continental, Oceanic and Planetary Flood Volcanism: American Geophysical Union Geophysical Monograph 100, p. 145–182, https://doi.org/10.1029/GM100p0145.

Kent, R.W., Kelley, S.P., and Pringle, M.S., 1998, Mineralogy and $^{40}Ar/^{39}Ar$ geochronology of orangeites (Group II kimberlites) from the Damodar Valley, eastern India: Mineralogical Magazine, v. 62, p. 313–323, https://doi.org/10.1180/002646198547701.

Kent, R.W., Pringle, M.S., Müller, R.D., Saunders, A.D., and Ghose, N.C., 2002, $^{40}Ar/^{39}Ar$ geochronology of the Rajmahal basalts, India, and their relationship to the Kerguelen Plateau: Journal of Petrology, v. 43, p. 1141–1153, https://doi.org/10.1093/petrology/43.7.1141.

Knight, K.B., Renne, P.R., Halkett, A., and White, N., 2003, $^{40}Ar/^{39}Ar$ dating of the Rajahmundry Traps, eastern India, and their relationship to the Deccan Traps: Earth and Planetary Science Letters, v. 208, p. 85–99, https://doi.org/10.1016/S0012-821X(02)01154-8.

Koppers, A.A.P., 2002, ArArCALC—Software for $^{40}Ar/^{39}Ar$ age calculations: Computers & Geosciences, v. 28, p. 605–619, https://doi.org/10.1016/S0098-3004(01)00095-4.

Kumar, A., and Ahmad, T., 2007, Geochemistry of mafic dikes in part of Chotanagpur gneissic complex: Petrogenetic and tectonic implications: Geochemical Journal, v. 41, p. 173–186, https://doi.org/10.2343/geochemj.41.173.

Le Maitre, R., Streckeisen, A., Zanettin, B., Le Bas, M., Bonin, B., and Bateman, P., eds., 2002, Igneous Rocks: A Classification and Glossary of Terms: Cambridge, UK, Cambridge University Press, 236 p., https://doi.org/10.1017/CBO9780511535581.

Mahadevan, T.M., 2002, Geology of Bihar and Jharkhand: Bangalore, India, Geological Society of India, 563 p.

Mahoney, J.J., 1988, Deccan Traps, *in* MacDougall, J.D., ed., Continental Flood Basalts: Dordrecht, Netherlands, Kluwer, p. 151–194, https://doi.org/10.1007/978-94-015-7805-9_5.

Mahoney, J.J., Jones, W.B., Fret, F.A., Salters, V.J.M., Pyle, D.G., and Davies, H.L., 1995, Geochemical characteristics of lavas from Broken Ridge, the Naturaliste Plateau and southernmost Kerguelen Plateau: Cretaceous plateau volcanism in the southeast Indian ocean: Chemical Geology, v. 120, p. 315–345, https://doi.org/10.1016/0009-2541(94)00144-W.

Mahoney, J.J., Duncan, R.A., Khan, W., Gnos, E., and McCormick, G.R., 2002, Cretaceous volcanic rocks of the South Tethyan suture zone, Pakistan: Implications for the Reunion hotspot and Deccan Traps: Earth and Planetary Science Letters, v. 203, p. 295–310, https://doi.org/10.1016/S0012-821X(02)00840-3.

McDonough, W.F., and Sun, S.-S., 1995, The composition of the Earth: Chemical Geology, v. 120, p. 223–253, https://doi.org/10.1016/0009-2541(94)00140-4.

McDonough, W.F., Sun, S.-S., Ringwood, A.E., Jagoutz, E., and Hofmann, A.W., 1992, K, Rb and Cs in the Earth and Moon and the evolution of the Earth's mantle: Geochimica et Cosmochimica Acta, v. 56, p. 1001–1012, https://doi.org/10.1016/0016-7037(92)90043-I.

Melluso, L., Srivastava, R.K., Petrone, C.M., Guarino, V., and Sinha, A.K., 2012, Mineralogy and magmatic affinity of the Jasra intrusive complex, Shillong Plateau, India: Mineralogical Magazine, v. 76, p. 1099–1117, https://doi.org/10.1180/minmag.2012.076.5.03.

Min, K., Mundil, R., Renne, P.R., and Ludwig, K.R., 2000, A test for systematic errors in Ar-Ar geochronology through comparison with U-Pb analysis of a 1.1-Ga rhyolite: Geochimica et Cosmochimica Acta, v. 64, p. 73–98, https://doi.org/10.1016/S0016-7037(99)00204-5.

Mukherjee, S., Misra, A.A., Calvès, G., and Nemčok, M., 2017, Tectonics of the Deccan large igneous province: An introduction, *in* Mukherjee, S., Misra, A.A., Calvès, G., and Nemčok, M., eds., Tectonics of the Deccan Large Igneous Province: Geological Society [London] Special Publication 445, p. 1–9, https://doi.org/10.1144/SP445.14.

Naqvi, S.M., and Rogers, J.J.W., 1987, Precambrian Geology of India: Oxford Monographs on Geology and Geophysics 6, 233 p.

Olierook, H.K.H., Jourdan, F., Merle, R.E., Timms, N.E., Kusznir, N.J., and Muhling, J., 2016, Bunbury Basalt: Gondwana breakup products or earliest vestiges of the Kerguelen mantle plume?: Earth and Planetary Science Letters, v. 440, p. 20–32, https://doi.org/10.1016/j.epsl.2016.02.008.

Olierook, H.K.M., Merle, R.E., and Jourdan, F., 2017, Toward a Greater Kerguelen large igneous province: Evolving mantle source contributions in and around the Indian Ocean: Lithos, v. 282–283, p. 163–172, https://doi.org/10.1016/j.lithos.2017.03.007.

Pande, K., 2002, Age and duration of the Deccan Traps, India: A review of radiometric and paleomagnetic constraints: Proceedings of the Indiana Academy of Sciences [Earth and Planetary Sciences], v. 111, p. 115–123.

Patil, S.K., and Arora, B.R., 2008, Palaeomagnetic and rock magnetic studies on the intrusives from Raniganj Basin, Damodar Valley: Linkage to the Rajmahal volcanic, *in* Srivastava, R.K., Sivaji, C., and Chalapathi Rao, N.V., eds., Indian Dikes: Geochemistry, Geophysics and Geochronology: New Delhi, India, Narosa Publishing House Pvt Ltd., p. 511–526.

Paul, D.K., 2005, Petrology and geochemistry of the Salma dike, Raniganj coalfield (Lower Gondwana), eastern India: Linkage with Rajmahal or Deccan volcanic activity?: Journal of Asian Earth Sciences, v. 25, p. 903–913, https://doi.org/10.1016/j.jseaes.2004.09.007.

Pyle, D.G., Christie, D.M., Mahoney, J.J., and Duncan, R.A., 1995, Geochemistry and geochronology of ancient southeast Indian Ocean and southwest Pacific Ocean seafloor: Journal of Geophysical Research, v. 100, p. 22261–22282, https://doi.org/10.1029/95JB01424.

Ramakrishnan, M., and Vaidyanadhan, R., 2010, Geology of India: Bangalore, Geological Society of India, 994 p.

Rekha, S., Upadhyay, D., Bhattacharya, A., Kooijman, E., Goon, S., Mahato, S., and Pant, N.C., 2011, Lithostructural and chronological constraints for tectonic restoration of Proterozoic accretion in the eastern Indian Precambrian Shield: Precambrian Research, v. 187, p. 313–333, https://doi.org/10.1016/j.precamres.2011.03.015.

Renne, P.R., Balco, G., Ludwig, K.R., Mundil, R., and Min K., 2011, Response to the comment by W.H. Schwarz et al. on "Joint determination of ^{40}K decay constants and $^{40}Ar^*/^{40}K$ for the Fish Canyon sanidine standard, and improved accuracy for $^{40}Ar/^{39}Ar$ geochronology" by P.R. Renne et al. (2010): Geochimica et Cosmochimica Acta, v. 75, p. 5097–5100, https://doi.org/10.1016/j.gca.2011.06.021.

Roy, A.B., 2004, The Phanerozoic reconstitution of Indian Shield as the aftermath of break-up of the Gondwanaland: Gondwana Research, v. 7, p. 387–406, https://doi.org/10.1016/S1342-937X(05)70792-9.

Rudnick, R.L., and Fountain, D.M., 1995, Nature and composition of the continental crust: A lower crustal perspective: Reviews of Geophysics, v. 33, p. 267–309, https://doi.org/10.1029/95RG01302.

Salters, V.J.M., Storey, M., Sevigny, J.H., and Whitechurch, H., 1992, Trace element and isotope characteristics of Kerguelen Plateau region, *in* Wise, S.W., Jr., et al., Proceedings of the Ocean Drilling Program, Scientific Results Volume 120, Par 1: Central Kerguelen Plateau: College Station, Texas, Ocean Drilling Program, p. 55–62.

Samal, A.K., Srivastava, R.K., Ernst, R.E., and Söderlund, U., 2019, Neoarchean–Mesoproterozoic mafic dike swarms of the Indian Shield mapped using Google™ Earth

images and ArcGIS™, and links with large igneous provinces, *in* Srivastava, R.K., Ernst, R.E., and Peng, P., eds., Dike Swarms of the World: A Modern Perspective: Singapore, Springer Geology, p. 335–390, https://doi.org/10.1007/978-981-13-1666-1_9.

Saxton, J.M., 2015, A method for measurement of ^{36}Ar without $H^{35}Cl$ interference: Chemical Geology, v. 409, p. 112–117, https://doi.org/10.1016/j.chemgeo.2015.05.017.

Schoene, B., Samperton, K.M., Eddy, M.P., Keller, G., Adatte, T., Bowring, S.A., Khadri, S.F.R., and Gertsch, B., 2015, U-Pb geochronology of the Deccan Traps and relation to the end-Cretaceous mass extinction: Science, v. 347, p. 182–184, https://doi.org/10.1126/science.aaa0118.

Schoene, B., Eddy, M.P., Samperton, K.M., Keller, B., Keller, G., Adatte, T., and Khadri, S.F.R., 2019, U-Pb constraints on pulsed eruption of the Deccan Traps across the end-Cretaceous mass extinction: Science, v. 363, p. 862–866, https://doi.org/10.1126/science.aau2422.

Sharma, R.S., 2009, Cratons and Fold Belts of India: Berlin, Springer-Verlag, 304 p.

Simonetti, A., Goldstein, S.L., Schmidberger, S.S., and Viladkar, S.G., 1998, Geochemical and Nd, Pb, and Sr isotope data from Deccan alkaline complexes—Inferences for mantle sources and plume-lithosphere interaction: Journal of Petrology, v. 39, p. 1847–1864, https://doi.org/10.1093/petroj/39.11-12.1847.

Singh, A.K., Chung, S.-L., Bikramaditya, R., Lee, H.-Y., and Khogenkumar, S., 2019, Zircon geochronology, Hf isotopic compositions and petrogenetic study of Abore volcanic rocks of Eastern Himalayan syntaxis, northeast India: Implications for eruption during breakup of eastern Gondwana: Geological Journal, https://onlinelibrary.wiley.com/doi/10.1002/gj.3477 (in press).

Sprain, C.J., Renne, P.R., Vanderkluysen, L., Pande, K., Self, S., and Mittal, T., 2019, The eruptive tempo of Deccan volcanism in relation to the Cretaceous-Paleogene boundary: Science, v. 363, p. 866–870, https://doi.org/10.1126/science.aav1446.

Srivastava, R.K., 1994, Petrology, petrochemistry and genesis of the alkaline rocks associated with the Ambadungar carbonatite complex, Baroda district, Gujarat, India: Journal of the Geological Society of India, v. 43, p. 23–39.

Srivastava, R.K., 1997, Petrology, geochemistry and genesis of rift-related carbonatites of Ambadungar, India: Mineralogy and Petrology, v. 61, p. 47–66, https://doi.org/10.1007/BF01172477.

Srivastava, R.K., 2011, Dike Swarms: Keys for Geodynamic Interpretation: Berlin, Springer-Verlag, 605 p., https://doi.org/10.1007/978-3-642-12496-9.

Srivastava, R.K., 2020, Early Cretaceous alkaline/ultra-alkaline and carbonatite magmatism in the Indian Shield—A review: Implications for a possible remnant of the Greater Kerguelen large igneous province: Episodes, Geodynamic Evolution of the Indian Sub-continent special issue (in press).

Srivastava, R.K., and Ahmad, T., 2008, Precambrian mafic magmatism in the Indian Shield—Part I: Journal of the Geological Society of India, Bangalore, v. 72, special issue 1, 140 p.

Srivastava, R.K., and Ahmad, T., 2009, Precambrian mafic magmatism in the Indian Shield—Part II: Journal of the Geological Society of India, Bangalore, v. 73, special issue 1, 152 p.

Srivastava, R.K., and Sinha, A.K., 2004a, The Early Cretaceous Sung Valley ultramafic–alkaline–carbonatite complex, Shillong Plateau, northeastern India: Petrological and genetic significance: Mineralogy and Petrology, v. 80, p. 241–263, https://doi.org/10.1007/s00710-003-0025-1.

Srivastava, R.K., and Sinha, A.K., 2004b, Geochemistry of Early Cretaceous alkaline ultramafic-mafic complex from Jasra, Karbi Anglong, Shillong Plateau, northeastern India: Gondwana Research, v. 7, p. 549–561, https://doi.org/10.1016/S1342-937X(05)70805-4.

Srivastava, R.K., and Sinha, A.K., 2007, Nd and Sr isotope systematics and geochemistry of plume-related Early Cretaceous alkaline-mafic-ultramafic-igneous complex from Jasra, Shillong Plateau, northeastern India, *in* Foulger, G.R., and Jurdy, D.M., eds., Plates, Plumes, and Planetary Processes: Geological Society of America Special Paper 430, p. 815–830, https://doi.org/10.1130/2007.2430(37).

Srivastava, R.K., Heaman, L.M., Sinha, A.K., and Shihua, S., 2005, Emplacement age and isotope geochemistry of Sung Valley alkaline-carbonatite complex, Shillong Plateau, northeastern India: Implications for primary carbonate melt and genesis of the associated silicate rocks: Lithos, v. 81, p. 33–54, https://doi.org/10.1016/j.lithos.2004.09.017.

Srivastava, R.K., Sivaji, C., and Chalapathi Rao, N.V., 2008a, Indian Dikes: Geochemistry, Geophysics and Geochronology: New Delhi, India, Narosa Publishing House Pvt Ltd., 650 p.

Srivastava, R.K., Sivaji, C., and Chalapathi Rao, N.V., 2008b, Indian dikes through space and time: Retrospect and prospect, *in* Srivastava, R.K., Sivaji, C., and Chalapathi Rao, N.V., eds., Indian Dike: Geochemistry, Geophysics and Geochronology: New Delhi, India, Narosa Publishing House Pvt Ltd., p. 1–18.

Srivastava, R.K., Chalapathi Rao, N.V.C., and Sinha, A.K., 2009, Cretaceous potassic intrusives with affinities to aillikites from Jharia area: Magmatic expression of metasomatically veined and thinned lithospheric beneath Singhbhum craton, eastern India: Lithos, v. 112, p. 407–418, https://doi.org/10.1016/j.lithos.2009.05.005.

Srivastava, R.K., Ernst, R.E., Hamilton, M.A., and Bleeker, W., 2010, Precambrian large igneous provinces (LIPs) and their dike swarms: New insights from high-precision geochronology, paleomagnetism and geochemistry: Precambrian Research, v. 183, special issue, p. 379–668.

Srivastava, R.K., Sinha, A.K., and Kumar, S., 2012, Geochemical characteristics of Mesoproterozoic metabasite dikes from the Chhotanagpur gneissic terrain, eastern India: Implications for their emplacement in a plate margin tectonic environment: Journal of Earth System Science, v. 121, p. 509–523, https://doi.org/10.1007/s12040-012-0172-z.

Srivastava, R.K., Kumar, S., Sinha, A.K., and Chalapathi Rao, N.V., 2014, Petrology and geochemistry of high-titanium and low-titanium mafic dikes from the Damodar Valley, Chhotanagpur gneissic terrain, eastern India, and their relation to mantle plume(s): Journal of Asian Earth Sciences, v. 84, p. 34–50, https://doi.org/10.1016/j.jseaes.2013.07.044.

Srivastava, R.K., Ernst, R.E., and Peng, P., eds., 2019a, Dike Swarms of the World: A Modern Perspective: Berlin, Springer-Verlag, 492 p., https://doi.org/10.1007/978-981-13-1666-1.

Srivastava, R.K., Guarino, V., Wu, F.-Y., Melluso, L., and Sinha, A.K., 2019b, Evidence of sub-continental lithospheric mantle sources and open-system crystallization processes from in-situ U-Pb ages and Nd-Sr-Hf isotope geochemistry of the Cretaceous ultramafic-alkaline-(carbonatite) intrusions from the Shillong Plateau, northeastern India: Lithos, v. 330–331, p. 108–119, https://doi.org/10.1016/j.lithos.2019.02.009.

Steiger, R.H., and Jäger, E., 1977, Subcommission on Geochronology: Convention on the use of decay constants in geo- and cosmochronology: Earth and Planetary Science Letters, v. 36, p. 359–362, https://doi.org/10.1016/0012-821X(77)90060-7.

Storey, M., Kent, R.W., Saunders, A.D., Salters, V.J., Hergt, J.M., Whitechurch, H., Sevigny, J.H., Thirlwall, M.F., Leat, P.T., Ghose, N.C., and Gifford, M., 1992, Lower Cretaceous volcanic rocks on continental margins and their relationship to the Kerguelen Plateau, *in* Wise, S.W., and Schlich, R., et al., Proceedings of the Ocean Drilling Program, Scientific Results Volume 120: College Station, Texas, Ocean Drilling Program, p. 33–53.

Wang, F., Jourdan, F., Lo, C.-H., Nomade, S., Guillou, H., Zhu, R.X., Yang, L., Shi, W., Feng, H., Wu, L., and Sang, H., 2014, YBCs: A new standard for $^{40}Ar/^{39}Ar$ dating: Chemical Geology, v. 388, p. 87–97, https://doi.org/10.1016/j.chemgeo.2014.09.003.

White, R.W., and McKenzie, D.P., 1989, Magmatism at rift zones: The generation of volcanic continental margins and flood basalts: Journal of Geophysical Research, v. 94, p. 7685–7729, https://doi.org/10.1029/JB094iB06p07685.

Widdowson, M., Pringle, M.S., and Fernandez, O.A., 2000, A post K-T boundary (early Palaeocene) age for Deccan-type feeder dikes, Goa, India: Journal of Petrology, v. 41, p. 1177–1194, https://doi.org/10.1093/petrology/41.7.1177.

Zhu, D.-C., Chung, S.-L., Mo, X.-X., Zhao, Z.-D., Niu, Y., Song, B., and Yang, Y.-H., 2009, The 132 Ma Comei-Bunbury large igneous province: Remnants identified in present-day southeastern Tibet and southwestern Australia: Geology, v. 37, p. 583–586, https://doi.org/10.1130/G30001A.1.

MANUSCRIPT RECEIVED 29 MAY 2019
REVISED MANUSCRIPT RECEIVED 16 SEPTEMBER 2019
MANUSCRIPT ACCEPTED 14 NOVEMBER 2019